Chapter 5

Strategies for the Design and Assembly of Hydrogen-bonded Aggregates in the Solid State

DONOVAN N. CHIN, JONATHAN A. ZERKOWSKI, JOHN C. MACDONALD AND GEORGE M. WHITESIDES
Department of Chemistry, Harvard University, Cambridge, MA, USA

1. INTRODUCTION

Crystalline organic materials are being actively explored for potential application in optoelectronics[1], and as piezoelectrics, photorefractives[2–4], and other types of functional materials. Macroscopic qualities (for example, non-linear optical coefficients, birefringence, toughness, and bioavailability) are important in specific applications[5,6]. To realize the potential of crystalline organic materials in materials science, it would be helpful to be able to correlate molecular structure, crystalline structure, and macroscopic properties to "design" materials: that is, to predict the crystalline packing of an organic compound based on its molecular structure, and to predict its macroscopic materials properties. In practice, chemists usually start their efforts to design materials at the level of molecular components, and build upwards in complexity. Strategies for this sort of molecular engineering, an endeavor we and others include under the broad term "non-covalent synthesis", are in their infancy[7–9].

Organised Molecular Assemblies in the Solid State Edited by James K. Whitesell

Predicting the packing of molecules in a crystal is difficult for several reasons. First, there are many possible arrangements of the molecules in space, and no algorithm exists that can sort though these alternatives efficiently. Second, polymorphism is a problem[10–16]. Organic molecules often pack in different crystalline arrangements that are nearly isoenergetic (within $\sim 1-2$ kcal/mol)[16], that is, in polymorphs. Third, polar groups contribute to this complexity by introducing long-range intermolecular electrostatic forces that compete with the short-range van der Waals forces[17]. Fourth, the competing kinetics of nucleation and crystal growth are poorly understood[18]. Crystallization may give crystals with structures that are determined primarily by kinetics rather than by thermodynamics.

One promising strategy for minimizing the complexity of the problem of correlating molecular and crystalline structure is to design the molecules so that they link into substructures through non-covalent intermolecular interactions. For several reasons, the hydrogen bond is well suited as an intermolecular connector for controlling the organization of organic molecules in solids. First, its directionality is well characterized[19,20]. Second, since the energy of a single hydrogen bond is relatively small (1–5 kcal/mol)[20–22] and molecules of polar solvent can compete for these donors and acceptors, formation of hydrogen bonds is reversible at room temperature. This reversibility permits practical experimental control over aggregation and growth of the lattice or its substructures. Third, a variety of organic functional groups can be used to introduce hydrogen-bonding capacity into a molecule. Finally, groups that form hydrogen bonds are compatible with many other functional groups[23,24]. These features recommend hydrogen bonds as elements with which to control structure in the organic solid state.

This chapter will examine ways in which hydrogen bonds have been used to rationalize, predict, or control structure in crystals of organic molecules. The first section will present an overview of studies (with emphasis on work of Etter) concerning selectivities of organic functional groups in forming hydrogen bonds, and the most common patterns of hydrogen bonds formed by these functional groups. These patterns can be used to design aggregates. The sections following review examples that have used hydrogen bonds to design crystalline arrays, including our own work with hydrogen-bonded aggregates based on substructures found in the cyanuric acid • melamine (CA • M) lattice. The final section briefly outlines the role of computational simulations in rationalizing and predicting structure in crystalline solids.

The strategies and examples reviewed here comprise one major current thrust in the field of crystal engineering[25,26]. This chapter does not provide a comprehensive overview of crystal engineering: we only consider those cases where the use of hydrogen bonding is the key strategy for design. This chapter also does not cover the fundamentals of hydrogen bonding or the geometrical statistics of hydrogen bonds in crystals, since there are already excellent

reviews on those topics[20]. Finally, we make no effort to categorize structures that contain hydrogen-bonded networks that were not the result of conscious efforts at design.

Other important topics, such as the modification of crystal habit by design of face-selective additives[27], and the investigation of reactivity in the solid state[28], are also outside the focus of this chapter.

2. SYSTEMATIC APPROACHES FOR DETERMINING PRINCIPLES AND RULES OF HYDROGEN BONDING

2.1 Patterns, Rules, and Selectivity of Hydrogen Bonds

The research of Etter focused in using hydrogen bonds to control the formation of molecular aggregates made up of small organic molecules containing limited sets of functional groups. Etter's approach is particularly valuable in that it relies on the intermolecular specificity of the hydrogen bonds rather than the size or shape of molecules to direct the formation of aggregates and to control their structure. These studies deliberately excluded competing factors such as preorganized cavities, ionic interactions, and steric interactions. This approach has permitted the evaluation of the independent contributions of hydrogen bonds to the structures of molecular aggregates. Her work can be categorized in three areas:

- characterization of patterns of hydrogen bonds in aggregates of small organic molecules using graph sets
- development of empirical rules that have been reasonably successful in predicting the connectivity of hydrogen bonds in molecular aggregates in the absence of other strong interactions
- determination of the selectivity of common organic functional groups in forming hydrogen bonds

2.1.1 Graph Sets

Etter recognized the need for a general and simple method for recognizing, characterizing, and comparing patterns of hydrogen bonds in molecular aggregates[29]. By applying graph theory to molecular aggregates, she broke down complex networks involving many different types of hydrogen bonds into simpler constituent motifs—that is, into subsets of molecules joined by just one type of hydrogen bond. Surprisingly, all patterns of hydrogen bonds can be broken down into just four simple motifs. Notation describing these motifs is assigned to each different type of hydrogen bond. This notation—referred to as a graph set—provides a complete and accurate description of the patterns of

hydrogen bonds in a network at any desired level of complexity[30]. Using graph-set analysis, networks containing many different types of hydrogen bonds have been described, and the similarities or differences in submolecular structure compared easily[31–34].

The process of assigning a graph set beings by identifying the different types of hydrogen bonds contained in a given network; these are determined by the molecular structures of the donors and acceptors[30]. The pattern formed by molecules connected to one another by just one type of hydrogen bond is called a *motif*. A motif is characterized by one of four *designators*. These designators are C(chain), R(ring), and D(dimer) for motifs generated from intermolecular hydrogen bonds. The designator S (self) denotes an intramolecular hydrogen bond. The number of donors and acceptors used in the motif are assigned as subscripts and superscripts respectively (which are dropped when both values are 1). The size of a motif (referred to as the *degree*) is determined by the number of atoms in a ring or the repeat unit of a chain, and is given in parentheses following the designator of the pattern. Figure 5.1 illustrates the procedure for assigning a graph set for the eight-membered ring formed by carboxylic acids. Examples of various motifs with their graph sets are shown in Figure 5.2[30]. The procedure for assigning graph sets has been reviewed recently by Bernstein *et al.*; the authors present many examples that clarify problems encountered frequently when assigning graph sets[34].

Analysis of graph sets can be employed in crystal engineering to identify isographic functional groups. Graph sets have been used systematically to identify patterns of hydrogen bonds that are common to different types of molecules or functional groups[31]. Functional groups that are isographic—that is, functional groups that are different structurally but that have the same graph set—contain the same number of donors and acceptors, and form

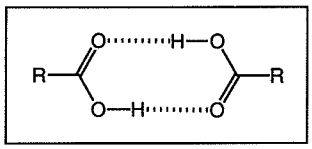

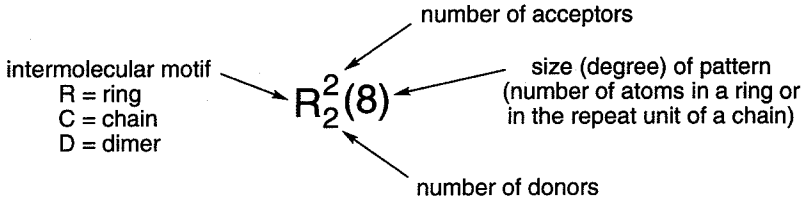

Figure 5.1 Components of a graph set. In this example, the graph set $R_2^2(8)$ is assigned to the ring motif formed by carboxylic acids.

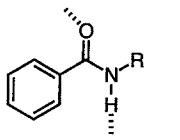

C(4) ≡ $C^1(4)$

1

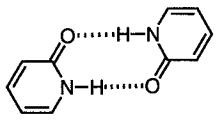

$R^2(8)$

2

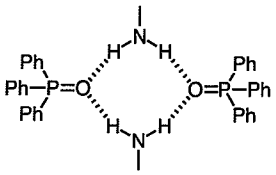

$R^2(8)$

4

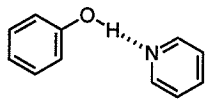

D ≡ $D^1(2)$

1

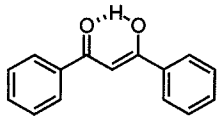

S(6)

Figure 5.2 Examples of different motifs of hydrogen bonds with their graph sets.

motifs in which molecules are connected by the same number of hydrogen bonds. Examples of several different isographic functional groups that form eight-membered rings (cyclic dimers) having the graph set $R_2^2(8)$ are shown in Figure 5.3.

The concept of isographic relationships provides a convenient method for designing structures in which several different molecular components having the same graph set can be interchanged. This approach has been used extensively by Etter in designing cocrystals. For example, one carboxyl groups of a dimer of carboxylic acids (Figure 5.3a) has been replaced by 2-amino-pyridine [45,46], amide[47,55], imide[50], and urea[51,52,56–58] moieties while preserving the $R_2^2(8)$ motif (Figures 5.3i–5.3l, respectively).

Graph sets also provide a basis for comparing patterns of hydrogn bonds in polymorphs. For example, five motifs occur in different combinations in three polymorphs of iminodiacetic acid ($—O_2CCH_2NH_2 + CH_2CO_2H$). Two

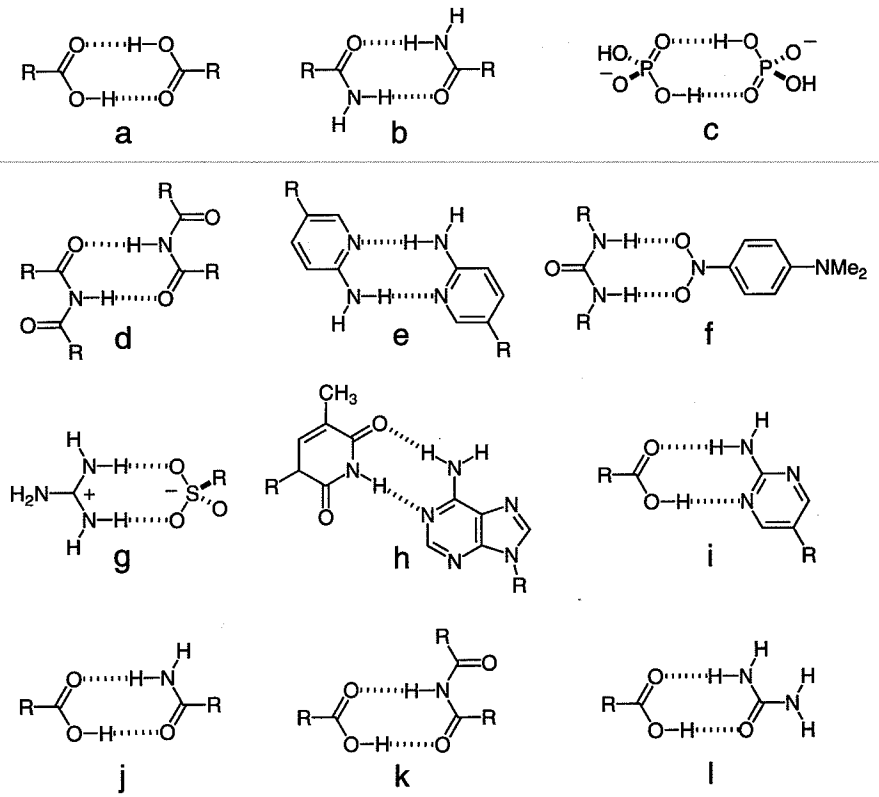

Figure 5.3 Isographic $R_2^2(8)$ motifs formed by (a) carboxylic acids[29,35], (b) primary amides[29,36], (c) anions of dihydrogen phosphate salts[37], (d) acyclic imides[38,39] (e) 2-aminopyridines[40], (f) bis(aryl)urea • N,N-dimethyl-*p*-nitroaniline cocrystal[41,42], (g) guanidinium sulfonate salts[43,44], (h) adenine • thymine base pair[20], (i) carboxylic acid • 2-aminopyrimidine cocrystals[45,46], (j) carboxylic acid • primary amide cocrystals[47–49], (k) carboxylic acid • acyclic imide cocrystals[50], and (l) carboxylic acid • urea cocrystals[51–54].

previous attempts have been made to distinguish these polymorphs based on their patterns of hydrogen bonds[59,60]. These analyses involved comparing geometries of bonds and relationships between the symmetry of neighboring molecules, as well as identifying several motifs consisting of hydrogen-bonded rings. Nevertheless, there was little understanding of the similarities between these structures or about the relative stabilities of the crystals. Structural differences were apparent immediately upon comparing the graph sets for these three structures[32,34]. Two polymorphs have the same graph sets for the first-level network (sum of all motifs), but the graph sets differ in their second-level networks (pattern involving two different types of hydrogen bonds, Figure 5.4).

Polymorph	Motifs	Networks
1	$C(5)R_2^2(10)C(8)$	$R_2^2(14)$
2	$C(5)R_2^2(10)C(8)$	$R_4^2(8)$
3	C(5)C(5)C(8)	

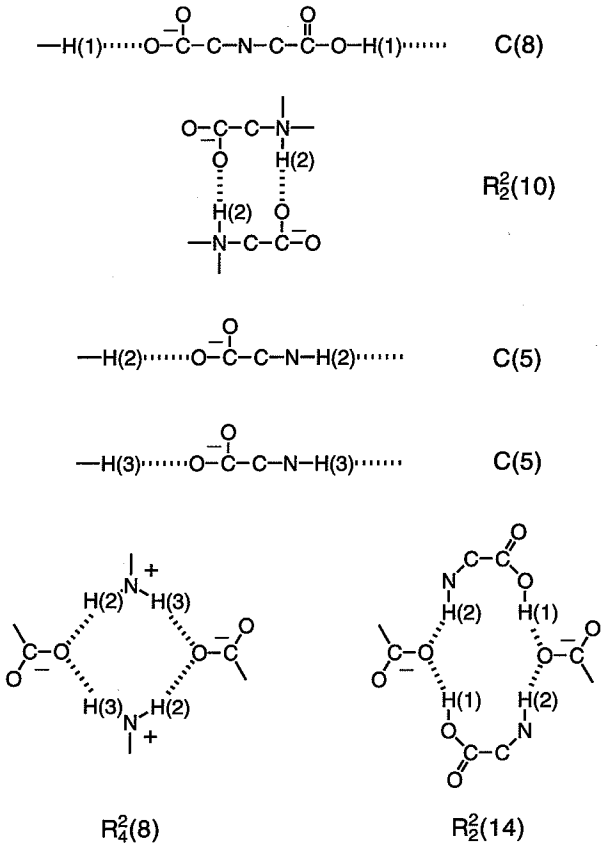

Figure 5.4 Graph set assignments for three polymorphs of iminodiacetic acid. Polymorph 3 differs from polymorphs 1 and 2 by the presence of a second C(5) motif. Polymorphs 1 and 2 are differentiated only when combinations of different kinds of hydrogen bonds (networks) are considered. These networks consist of rings of different sizes.

Computational routines that perform graph set analysis are presently being incorporated into the Cambridge Structural Database (CSD). Graph sets are being used with increasing frequency to design and analyze the structures of aggregates[34]. The CSD presently contains data from $> 10^5$ crystal structures[61]. Using automated algorithms, investigators can in principle, generate, visualize, and compare graph sets for large numbers of crystals structures. Employing graph sets in this manner aids in establishing relationships between the structure of hydrogen-bonded aggregates, and in determining how this structure affects the properties of organic solids.

2.1.2 Rules for Hydrogen Bonds

Etter analyzed the graph sets of a large number of crystal structures to determine distributions of graph sets for classes of molecules containing one particular functional group, and, conversely, distribution of functional groups for structures with a particular graph set[31,33]. Empirical rules of hydrogen bonding are one way to use correlations between functional groups and their patterns of hydrogen bonds, with graph sets being one type of correlation. Graph sets describe the connectivity or configuration of aggregates composed of hydrogen-bonded molecules. Other structural or stereoelectronic factors affecting the primary, secondary, or even tertiary structure of aggregates provide other rules of hydrogen bonding[31].

Three rules with broad but not universal generality for hydrogen bonds that apply to functional groups in neutral organic molecules are: (i) all good proton donors and acceptors are used in hydrogen bonding; (ii) intramolecular hydrogen bonds that form a six-membered ring will occur in preference to intermolecular hydrogen bonds; and (iii) the best proton donors and acceptors remaining after formation of intramolecular hydrogen bonds form intermolecular hydrogen bonds to one another. Additional rules for specific classes of functional groups have been determined, but will not be discussed here[31].

Rules of this sort reflect energetically favorable modes of intermolecular association that occur frequently in the packing patterns of organic crystals. Expected patterns of hydrogen bonds might not occur, however, for a variety of reasons. These reasons include steric effects[62], the presence of multiple sites for hydrogen bonding[63], and competing ionic forces[64]. Examples of such systems are shown in Figure 5.5.

In some cases, different motifs of hydrogen bonds occur by alternative connection of the same set of donors and acceptors; these motifs can give rise to different polymorphic crystalline forms. The patterns of hydrogen bonds found in two polymorphs of diacetimide[65,66] and three polymorphs of 5,5-diethylbarbituric acid[67,68] are shown in Figure 5.6. These examples illustrate that rules of hydrogen bonding cannot always predict which pattern will form

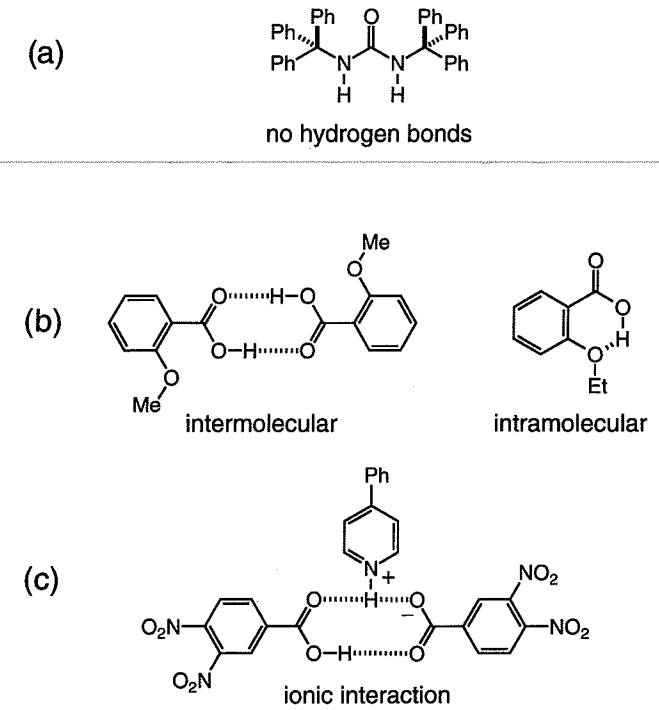

Figure 5.5 Molecules or aggregates that form unexpected patterns of hydrogen bonds. (a) Molecules of ditritylurea do not form intermolecular hydrogen bonds to one another because the urea groups are sterically inaccessible. (b) Molecules of *o*-methoxybenzoic acid form the expected dimer motif of carboxylic acids, while molecules of *o*-ethoxybenzoic acid form an intramolecular hydrogen bond. (c) The cocrystalline complex between 3,4-dinitrobenzoic acid and 4-phenylpyridine forms an unusual ring motif involving one neutral acid and a pyridinium–carboxylate pair.

when molecules can pack in several arrangements that are close in energy ($\sim 1-2$ kcal/mol)[16].

Studies of hydrogen bonding in organic crystals have shown that certain classes of functional groups almost always form hydrogen bonds when complementary donors or acceptors are available, while other classes of functional groups only occasionally participate in hydrogen bonding. Examples of functional groups that have been classified (loosely) by Etter as good or poor donors and acceptors are shown in Figure 5.7.

The concept of the best donor and acceptor forming a hydrogen bond provides a powerful tool for controlling the composition and structure of molecular aggregates in a crystal. For instance, Etter[48,55,69] and Lechat[70,71] have designed molecular complexes that are supramolecular analogs of nitroanilines by using complementary sets of strong and weak hydrogen bonds

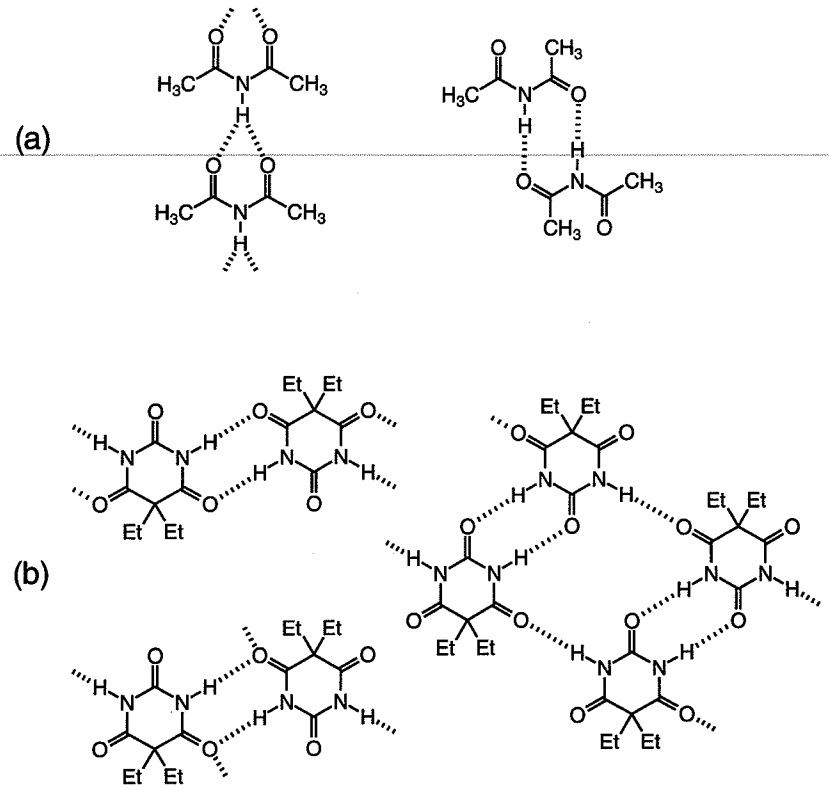

Figure 5.6 The patterns of hydrogen bonds found in (a) two polymorphs of diacetimide and (b) three polymorphs of 5,5-diethylbarbituric acid.

to assemble the molecular components. Examples of cocrystalline supramolecular analogs of *m*-nitroaniline and 3,5-dinitroaniline are illustrated in Figures 5.8 and 5.9, respectively. In each case, the amino and nitro groups were placed on separate molecules and then linked via strong O—H···O interactions to give heterodimers. Formation of a second, weaker set of N—H···O interactions between the amino and nitro groups preserved the patterns of hydrogen bonds (chains or layers) formed by the parent compound. The proposed structure of 3,5-dinitroaniline is believed to be a layer (Figure 5.10) although attempts to solve the crystal structure of this compound have been unsuccessful due to twinning of the crystals.

One of the conditions usually necessary for second-order nonlinear optical properties to occur is that the bulk material has no center of symmetry[72]. The cocrystals in Figures 5.8 and 5.9 demonstrate the use of hydrogen bonds to form one- and two-dimensional structures (chains and layers) that lack a center of

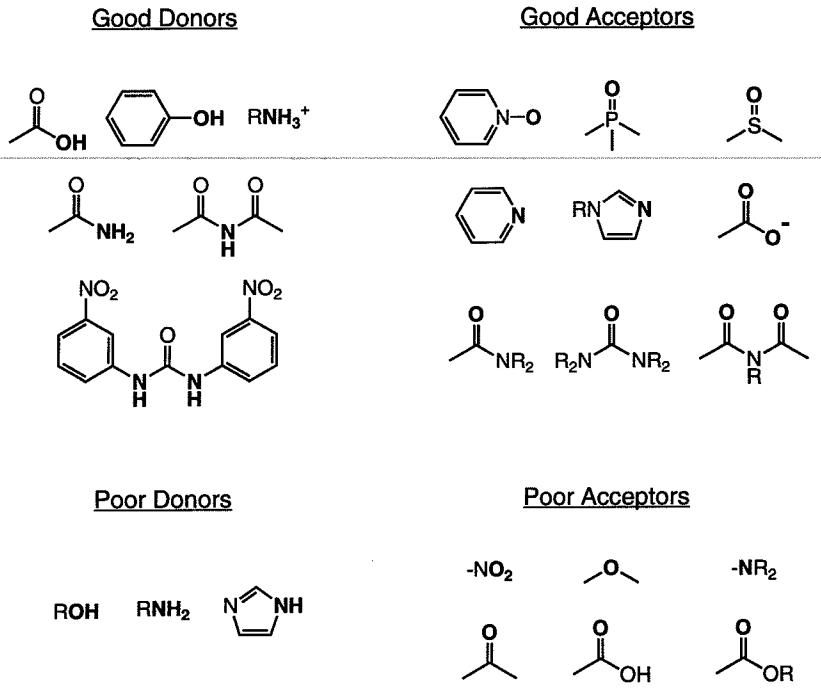

Figure 5.7 Examples of functional groups that form hydrogen bonds in organic crystals. Good donors and acceptors almost always participate in hydrogen bonding, while poor donors and acceptors only occasionally form hydrogen bonds.

symmetry. The layer motif shown in Figure 5.11 is one example in which the final bulk structure of the crystal was found to be acentric[55]. The polar layers of molecules in this structure are parallel and unidirectional, although the nature of the interplanar interactions in this crystal is not clear.

2.1.3 Selectivity of Functional Groups in Forming Hydrogen Bonds

Selectivity of organic functional groups has been determined from studies of competition between a single acceptor (A) for multiple donors (D), and vice versa. Relative abilities of various functional groups in forming hydrogen bonds were determined by examining which donors and acceptors are actually used to form hydrogen bonds, and with what frequency, in crystals. Such studies do not measure the thermodynamic or kinetic contributions of hydrogen bonds to the formation of a particular crystal structure; rather, they determine whether functional groups show consistent patterns of selectivity in the solid state. The extent to which these patterns match those found in solution (or in the gas

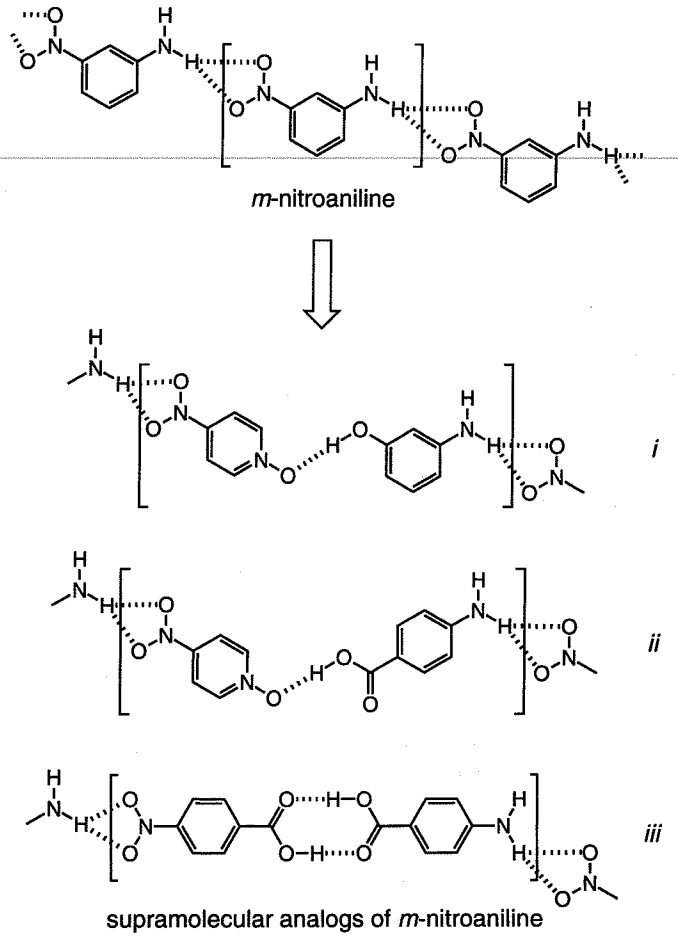

Figure 5.8 Hydroxy, N-oxide, and carboxylic acid functional groups (i–iii) have been used to join aniline and nitrobenzene rings to create extended supramolecular analogs of *m*-nitroaniline.

phase) reflects the degree with which the strengths of hydrogen bonds at equilibrium determine the structures of aggregates in the solid state.

Three general schemes for ranking functional groups are shown in Scheme 5.1. In each case, two different donors compete in forming a hydrogen bond with a single acceptor. Scheme 5.1i represents crystallization of a single-component system where the donors and acceptor reside on the same molecule. Scheme 5.1ii represents cocrystallization between two components, a molecule with two donors and a second molecule with one acceptor. Scheme 5.1iii involves cocrystallization between three components. In this experiment, a

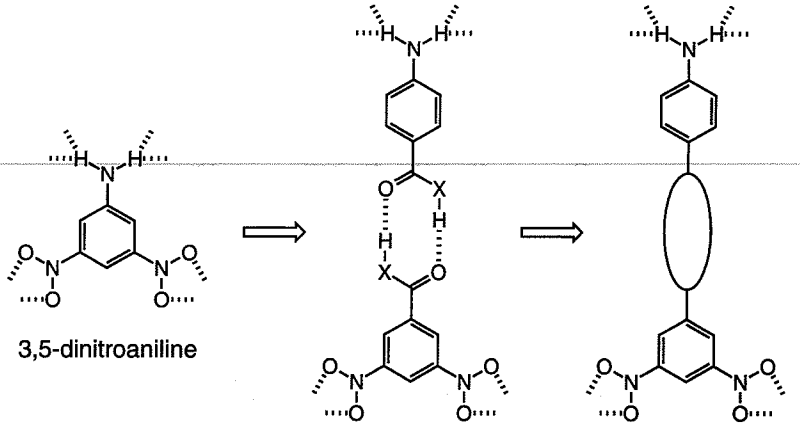

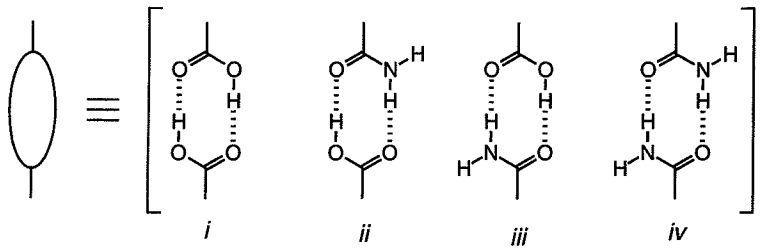

Figure 5.9 Carboxylic acid and amide functional groups (i–iv) have been used to join aniline and dinitrobenzene rings to create extended supramolecular analogs of 3,5-dinitroaniline.

molecule with an acceptor selects one of two different molecules, each containing a single donor, during crystallization. Examples of each of these types of experiment are described below.

Cocrystals of pyridines with benzonic acids. Etter found that experiments involving competitive cocrystallization of a single acceptor with several different, competitive donors (Scheme 5.1iii) provide a convenient method for evaluating the donating (or accepting) ability of functional groups. For example, 4-phenylpyridine and ethyl isonicotinate were both capable of complexing and completely separating the acid of lower pK_a value from a second acid is higher pK_a value by cocrystallization (Figure 5.12)[33]. Even acids with pK_a values that are close to one another, such as 3,4-dinitro- and 3,5-dinitrobenzoic acid ($\Delta pK_{acalc} = 0.04$), were cleanly separated using this technique. These experiments imply that the strength of the hydrogen bond in solution—to the

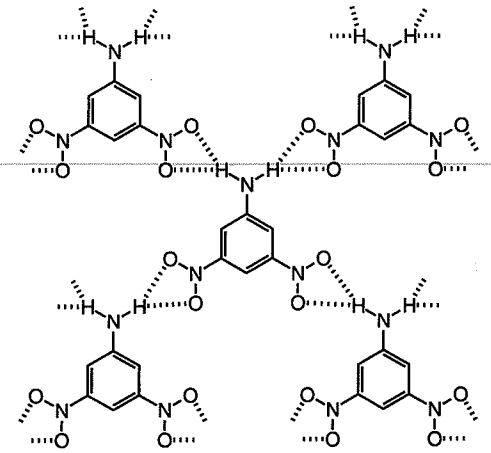

Figure 5.10 The proposed two-dimensional pattern of hydrogen bonds (layer) formed by molecules of 3,5-dinitroaniline.

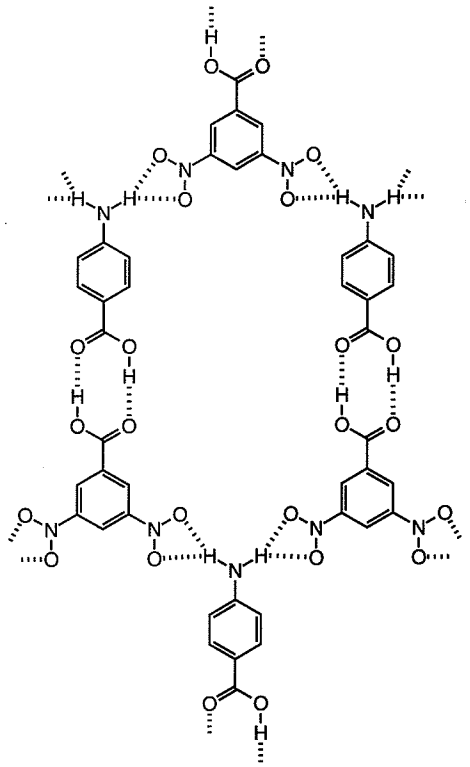

Figure 5.11 Polar layer of molecules found in the cocrystal between 4-aminobenzoic acid and 3,5-dinitrobenzoic acid. The nitro and aniline groups form the same patterns of hydrogen bonds found in the crystal structures of nitroanilines.

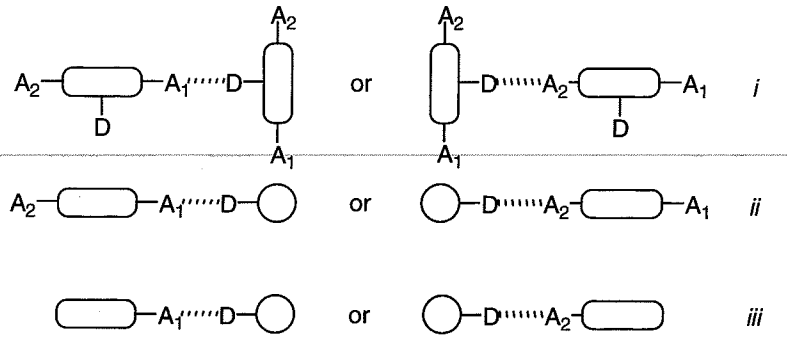

Schemes 5.1 Three general schemes (i–iii) for evaluating the relative abilities of donors (D) and acceptors (A) in forming hydrogen bonds based on competition between functional groups during crystallization.

extent that pK_a values reflect this parameter—determines which aggregate will nucleate the growth of crystals, even when the difference in strength (pK_a value) is small.

Cocrystals with acyclic imides. Acyclic imides formed cocrystals with a variety of guest molecules such as ureas, carboxylic acids, amides, and phenols[50]. In the absence of a guest, acyclic imides crystallized either as chains or dimers (Figure 5.13), depending on the steric bulk of substituents R[38,39]. Guest molecules readily formed complexes with acyclic imides, giving cocrystals with the different motifs (Figure 5.13b). A pattern that recurred frequently when acyclic imides crystallized with phenols was one in which the imide dimer was preserved, and in which the two remaining carbonyl groups were used to bond to the OH groups of phenol. This arrangement is illustrated schematically in Figure 5.14. Etter demonstrated that phenols with two OH groups, such as hydroquinone, could be used to join imide dimers into infinite chains.

Cocrystals of 2-aminopyrimidine with carboxylic acids. Studies of cocrystallization between 2-aminopyrimidines (2AP) and mono- or dicarboxylic acids have shown that selectivity during the formation of cocrystals can be used to monitor subtle changes in the abilities of functional groups to accept hydrogen bonds arising from the effect of substituents. Carboxylic acids, for example, cocrystallized with 2APs to form complexes with ratios (2AP:acid) of 1:2, 1:1, and 2:1, as shown in Figure 5.15[45,46]. The stoichiometry of the cocrystal was controlled, in part, by the ratio of starting materials used. Several carboxylic acids showed a single preferred stoichiometry of 1:1, however, regardless of the ratio of starting materials or of the method of preparation.

Cocrystals with triphenylphosphine oxide (TPPO). Etter has demonstrated that TPPO forms complexes in the solid state with a wide variety of molecules, examples of which are shown in Figure 5.16[48,73]. These complexes were

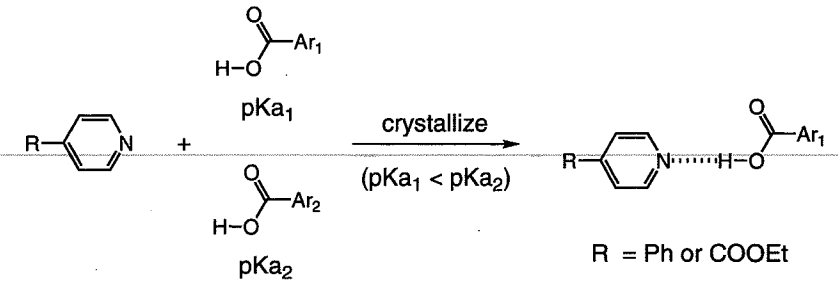

Acid in Cocrystal Ar_1COOH	ΔpKa	Uncomplexed Acid Ar_2COOH
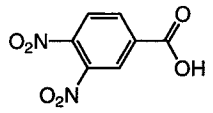	2.35	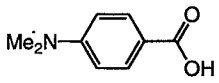
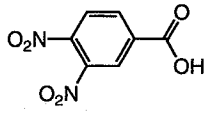	0.74	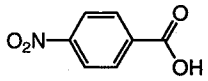
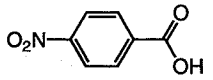	0.41	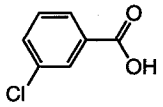
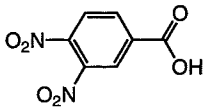	0.04	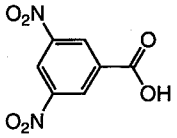

Figure 5.12 Strongly hydrogen-bonded pyridine • benzoic acid dimers were found in cocrystals formed selectively in the presence of a second weaker (higher pK_a) benzoic acid.

stabilized by strong hydrogen bonds between the phosphoryl oxygen and an acidic hydrogen on the guest. This interaction was present in every structure, despite the presence of additional heteroatoms that could compete with TPPO in forming a hydrogen bond. In most cases, the substrates formed chains of hydrogen bonds when crystallized in the absence of TPPO. Complexation of the guest by TPPO usually gave dimers or tetramers (Figure 5.17).

The complexes of TPPO generally formed large, well-developed crystals, while many of the starting materials formed thin needless. Etter suggested that

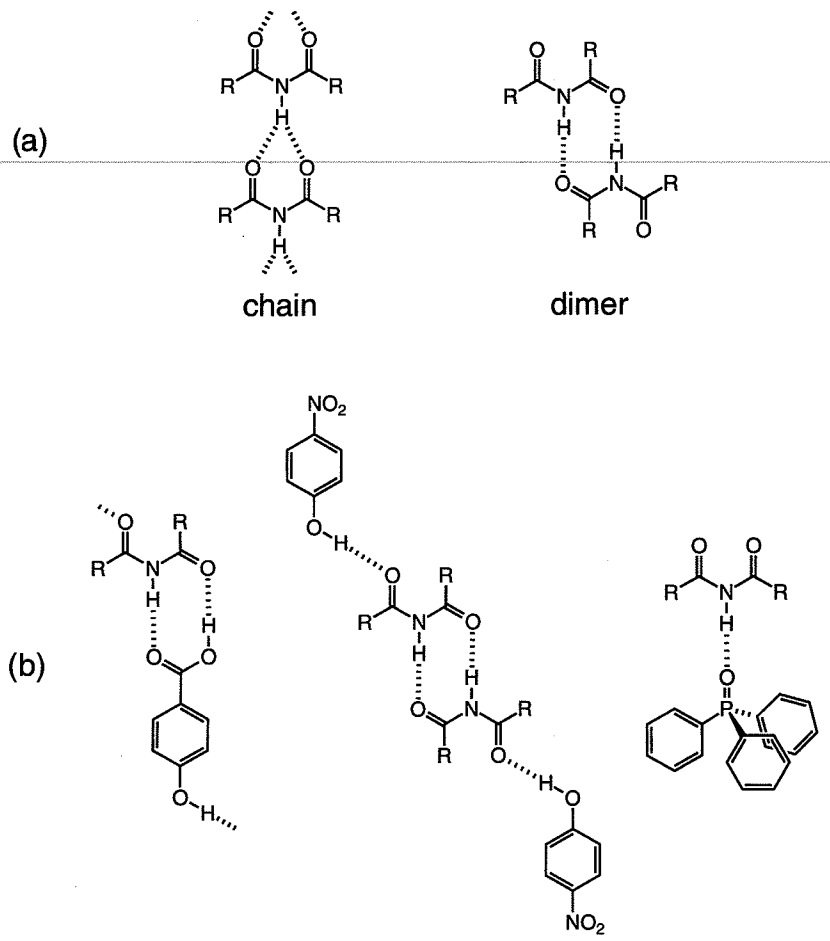

Figure 5.13 (a) Two motifs (chains and dimers) formed by acyclic imides. (b) Cocrystalline complexes formed between acyclic imides and guest molecules having good proton donors and acceptors.

two factors contribute to the effect that TPPO has on the growth of crystals: one is the presence of a strong hydrogen bond that imparts partial ionic character to the crystal; the other is the bulky shape of TPPO, which inhibits the formation of lamellar structures that often induce crystals to grow as thin plates or needles.

Cocrystals with 1,3-bis(m-nitrophenyl)urea (MNPU). Studies of cocrystallization of bis(aryl)ureas with a variety of guest molecules have shown that MNPU, in particular, is capable of forming hydrogen-bonded complexes with molecules containing proton acceptors[41,42]. Examples of several such complexes are shown in Figure 5.18. Guest molecules with strong acceptors

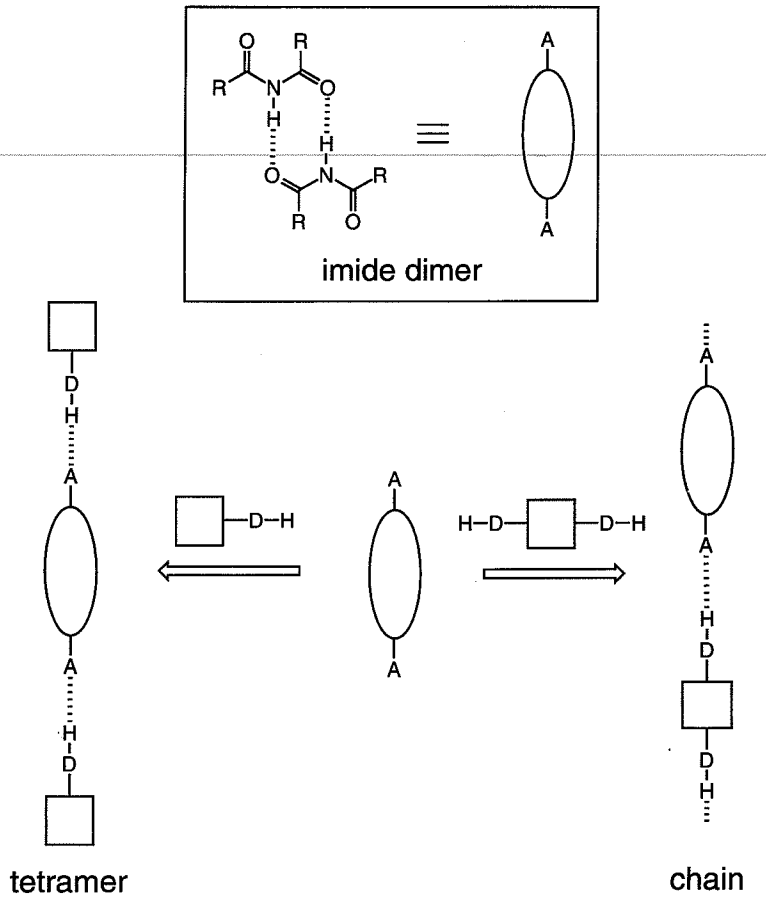

Figure 5.14 Schematic representation of motifs formed by acyclic imides. Acyclic imides that form cyclic dimers (top) have one carbonyl group that is not used in hydrogen bonding. The unbonded carbonyl groups of these dimers serve as sites for hydrogen bonding to molecules that are proton donors (bottom).

such as phosphine oxides and sulfoxides, as well as those with much weaker acceptors such as nitro, ketone, and ether groups, formed complexes in the solid state.

The ability of MNPU to form cocrystals differed from that of other bis(aryl)ureas in several ways. The oxygen of the carbonyl group formed two intramolecular C—H···O interactions with the aryl hydrogens *ortho* to the nitro groups; these weak interactions stabilize the molecule in a planar conformation. In this conformation, the carbonyl group generally did not participate in intermolecular hydrogen bonding. Thus, MNPU is a rare example

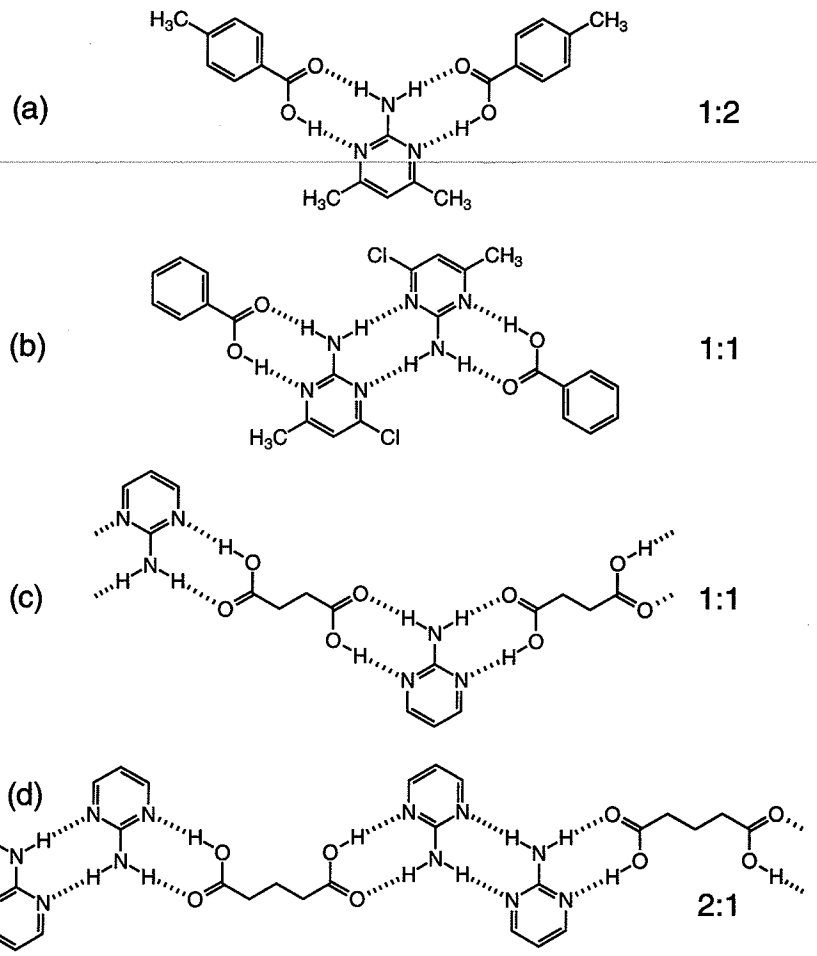

Figure 5.15 Motifs formed in cocrystals with different stoichiometries (pyrimidine:acid) of 2-aminopyrimidines and mono- or dicarboxylic acids.

of a neutral organic molecule that acts solely as a proton donor. Such species are rare because heteroatoms covalently bonded to acidic hydrogen atoms are almost always involved in hydrogen bonding, as stated previously.

Stereoelectronic preferences of functional groups. Etter's work has also demonstrated that stereoelectronic preferences of functional groups can affect the structure of aggregates, especially in crystals containing molecules with a limited number of donors and acceptors and with no other strong intermolecular interactions. The best example of this phenomenon can be seen in the crystal structures of 1,3-cyclohexanediones. These molecules have one donor and one

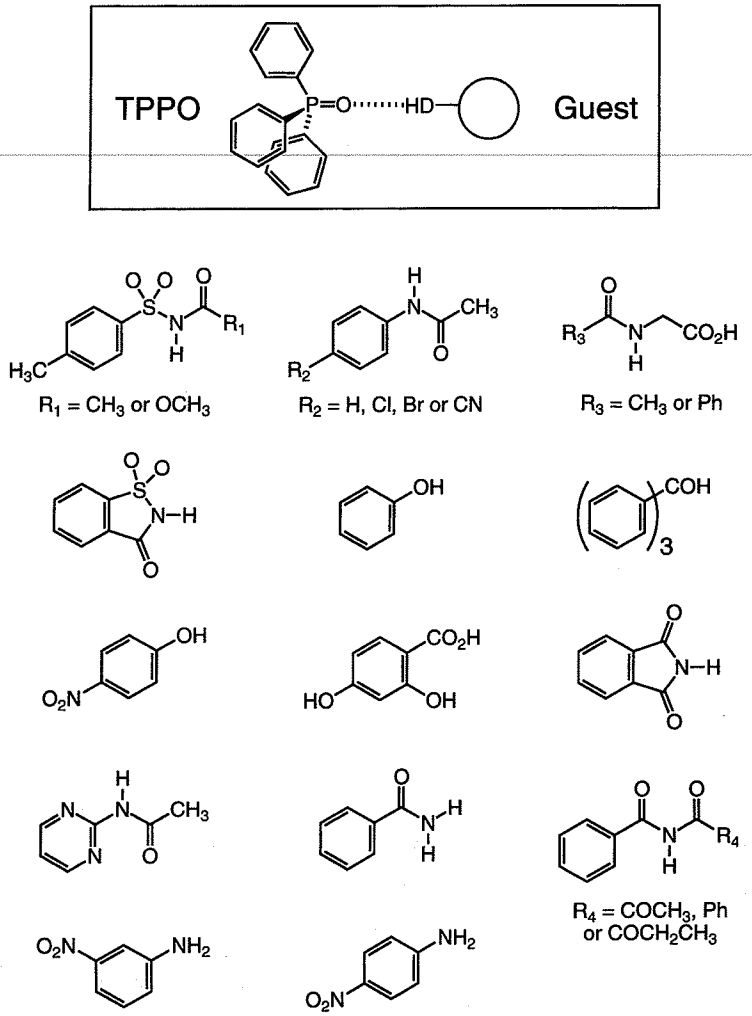

Figure 5.16 Examples of guest molecules that crystallize as hydrogen-bonded host–guest complexes with triphenylphosphine oxide (TPPO).

acceptor. Four stereochemically characteristic modes of association can arise from two different planar conformations of the OH group, and form the choice of *syn* or *anti* lone pairs of electrons on the carbonyl group as the site of the acceptor (Figure 5.19). Energetic preferences for the different modes of association may differentiate cyclic and linear aggregates energetically. The *syn–syn* motif was observed in the crystal structure for 5,5-dimethyl-1,3-cyclohexanedione[74,75], the *anti–anti* motif for 1,3-cyclohexanedione (CHD)[76],

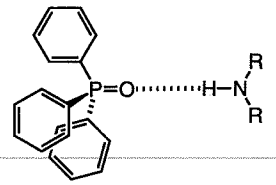

dimer

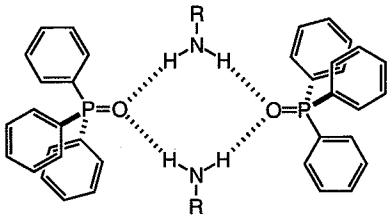

tetramer

Figure 5.17 Dimer and tetramer motifs found frequently in cocrystals with TPPO.

and the *syn-anti* motif (with a molecule of benzene trapped in the center of the central cavity) for both CHD and 5-methyl-1,3-cyclohexanedione[77]. The cyclic structure—referred to as a *cyclamer*—is similar to that of crown ethers with a hydrogen-bonded rather than a σ-bonded backbone. Etter demonstrated that cyclamers of CHD are able to trap molecules of benzene and thiophene selectively during crystallization.

2.2 Weak Hydrogen Bonds (C—H···O) as Steering Interactions

Desiraju convincingly demonstrated that hydrogen bonds other than those taking part in strong XH···X interactions (X=O and N) can play an important role in determining crystal packing[78–81]. For example, the acidity of the CH donor group again appears to be important in determining the strength of CH···O interactions[82]. Desiraju developed a "crystallographic scale of carbon acidity" in which C···O distances appear to correlate with the acidity of the CH group (as measured independently in DMSO)[83]. Two different correlations emerge; those for CH donors that are sterically hindered, and those for CH donors that are unhindered. The importance of hybridization at the carbon in determining the strength of C—H···O interactions is evident in comparing alkynes with alkenes. For example, Desiraju showed that alkynes form shorter C···O contacts (3.46 Å on average), while alkenes form longer contacts (3.46 Å on average)[84]. While this difference in lengths (0.18 Å) is small, the majority of the shortest contacts (3.1–3.4 Å) involve alkynes.

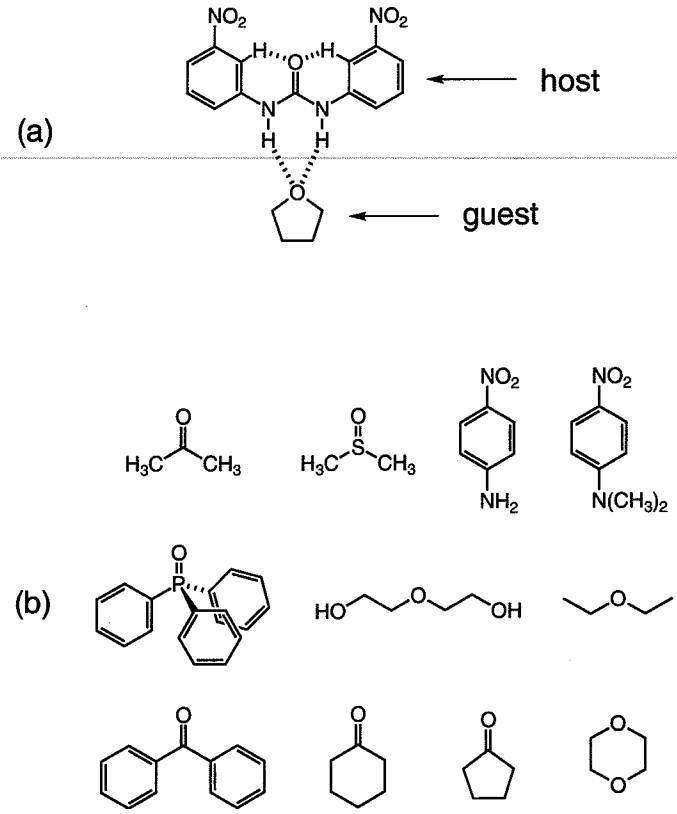

Figure 5.18 (a) Hydrogen-bonded complex between 1,3-bis(*m*-nitrophenyl)urea (host) and tetrahydrofuran (guest). (b) Examples of other guest molecules that form complexes with 1,3-bis(*m*-nitrophenyl)urea.

Desiraju also studied other C—H···O interactions in compounds containing chlorine atoms to determine how electronegative groups affect the acidity of CH hydrogens[82]. The average C···O distances for structures in the series Cl_3CH, Cl_2RCH,ClR_2CH, and R_3CH were 3.32 Å, 3.40 Å, 3.46 Å, and 3.59 Å respectively; thus, in this series, the length of C—H···O interactions varied directly with the number of attached chlorine atoms. Another type of weak interaction studied by Desiraju was XH···C(X=O and N; referred to as a π hydrogen bond) where the acceptor was an alkyne, alkene, or phenyl group[85]. In these studies, the average H···C distances were significantly less than the sum of van der Waals radii for C and H atoms (2.95 Å): observed values ranged from 2.43 Å for OH···C_{phenyl} to 2.82 Å for NH···C_{alkene} contacts.

The work of Desiraju suggests that the more acidic the CH hydrogen involved in a C—H···O interaction is (and therefore the stronger the interaction), the

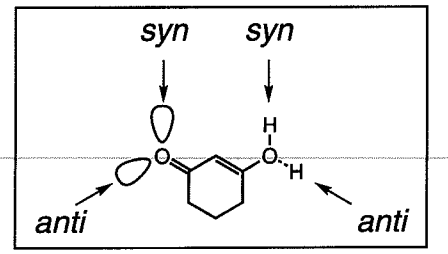

(a) *syn-syn*

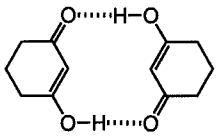

(b) *anti-anti*

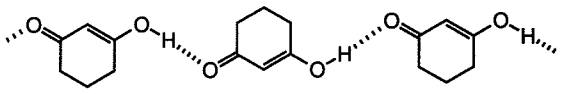

(c) *syn-anti*

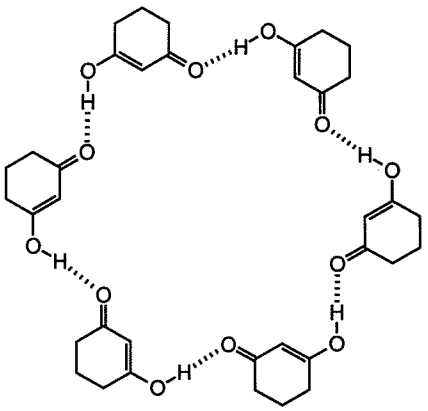

Figure 5.19 Four stereoelectronically different motifs of 1,3-cyclohexanediones are shown. Structures a–c have been found in the crystal structures of cyclohexanedione molecules with different substituents. Structure c crystallizes with molecules of benzene included in the central cavity of the crown-ether-like ring.

(d) *anti-syn*

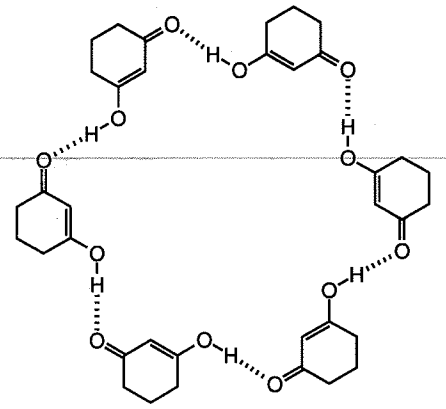

Figure 5.19 (*contd.*)

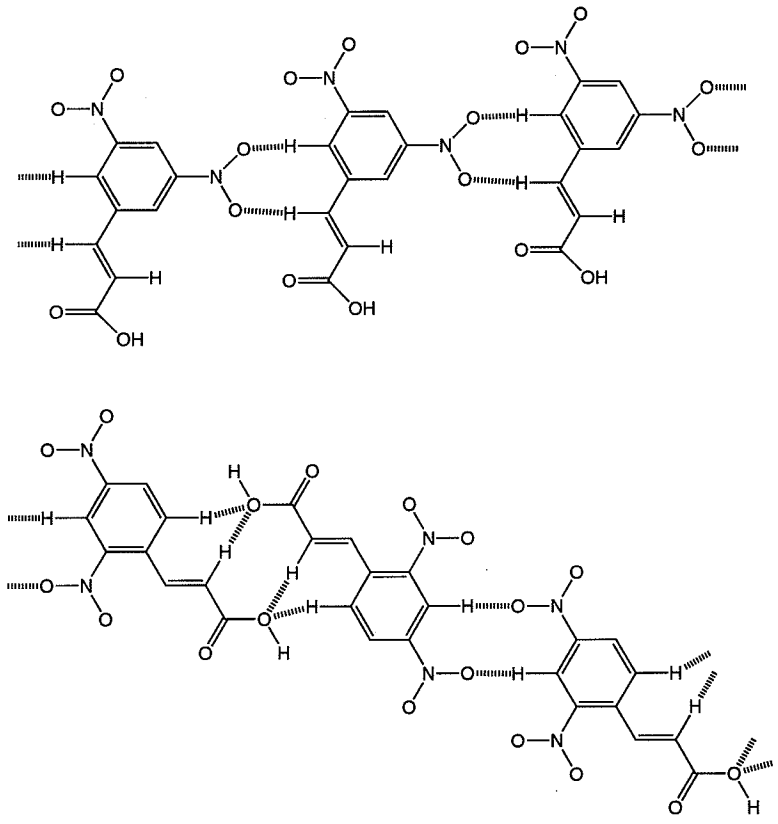

Figure 5.20 Two chain motifs of dinitrocinnamic acids. The top motif is built from one type of CH···O interaction, while that at the bottom uses two different types of CH···O contacts.

more useful thus interaction will be in designing structures. For example, he has used hydrogen bonds involving the alkene protons of cinnamic acids[86], and the aromatic protons of nitroaromatic compounds[87,88] to engineer the structures of crystals. Figure 5.20 shows two recurring patterns formed by these moieties. CH···O interactions are the only type of hydrogen bonds present in both patterns, one of which involves two different hydrogen-bonding motifs to link adjacent molecules in a chain. Another interesting structure involves COOH dimers alternating with an approximately isostructural pattern between dimethylamino and nitro groups to produce a chain of molecules (Figure 5.21).

This last example indicates that these weak CH···O interactions can occur alone in a crystal or in conjunction with stronger hydrogen bonds. In the latter case, Etter's guideline is followed: the structure can be rationalized by assuming that the strongest donors and acceptors pair first, followed by pairing of weaker donors and acceptors. In other words, the geometric demands of stronger hydrogen-bonding moieties usually determine which motifs form (e.g. the uniquitous carboxylic acid dimer), while weaker hydrogen bonds such as CH···O interactions determine how these aggregates pack into higher order aggregates such as stacks or layers. In some cases the weaker hydrogen bonds can influence the type of motif adopted by the strong hydrogen bonds. For example, Desiraju showed that a cocrystal between two carboxylic acids containing no CH···O interactions was dominated by π–π interactions. These π–π forces promote the formation of homodimers between the two carboxylic acids rather than heterodimers, as predicted purely on the strengths of OH···O hydrogen bonds, and the principle that the best donor and acceptor, which reside on different acids, will pair first[89]. This example illustrates one of Desiraju's key points: to control or rationalize crystalline supermolecular architecture, weak interactions—both hydrogen bonds and other kinds—must be taken into consideration[82,90,91].

Desiraju demonstrated the importance of CH···O interactions in controlling molecular packing in a series of experiments. These experiments showed that aromatic hydrocarbons pack almost exclusively in different structural categories depending on the ratio of carbon to hydrogen (C : H): herringbone patterns

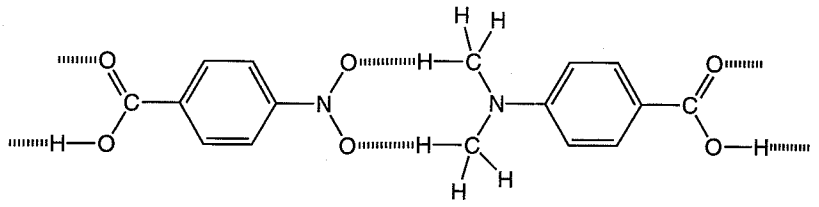

Figure 5.21 A hydrogen-bonded chain held together by CH···O contacts between dimethylamino and nitro groups, as well as by carboxylic acid dimers.

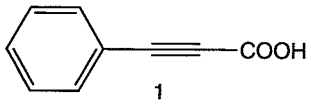

1

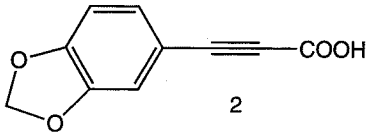

2

Figure 5.22 The added oxygen atoms in **2** allow the formation of intermolecular CH···O contacts that favor adoption of a stacked, sheet-like packing arrangement, whereas **1** packs as dimers that adopt a herringbone motif.

(called β-structures) at low C:H ratios; columns and sheets at high C:H ratios[78,82,92]. Desiraju reasoned that adding oxygen atoms to the molecules would promote the formation of CH···O bonds—that is, the hydrogen atoms would be less likely to engage in the H···C contacts necessary for herringbone packing—thus increasing the effective C:H ratio, and driving the molecules to pack in the β-structure (Figure 5.22). Desiraju also reasoned that intermolecular CH···O contacts should favor formation of layered structures. Experimentally, a higher content of oxygen led to packing in stacks and layers. This work has practical ramifications for reactivity in the solid state. For example, stacked acetylene groups exhibit thermal reactivity as diene/dienophile pairs for cycloaddition reactions in the solid state[82,92,93].

2.3 Resonance-Assited Hydrogen Bonding (RAHB)

Gilli's group has shown, using surveys of the crystallographic database as well as their own experimental results, that the strengths of hydrogen bonds are intimately related to electronic features of the molecules involved[94–97]. Their Resonance-Assited Hydrogen Bonding (RAHB) model states that there is "synergistic coupling between the increased π- resonance and hydrogen-bond strengthening"[94]. While most of their examples are based on intramolecular hydrogen bonding (which is outside the scope of this review) particularly in β-diketone enols or related structures, they have also shown that the phenomenon is relevant to intermolecular hydrogen bonding. The key feature of their model is that a change-separated resonance form enhances hydrogen bonding when they hydrogen-bonded groups are conjugated (see **3** and **4**). The extent of resonance or delocalization can be quantified by a parameter derived from bond lengths along the conjugted backone. This parameter does correlate

with the strength of the hydrogen bond, as measured by the intermolecular oxygen–oxygen distance and the length of the covalent O—H bond. That electronic effects are important is shown by structures of ketoesters, which form longer hydrogen bonds than diketones: electron donation from the extra ester oxygen disfavors the charge-separated resonance form (**3**) that would otherwise enhance hydrogen bonding[95]. This opposition of inductive and resonance effects also arises in intramolecular cases, notbaly in *para*-substituted diketo-arylhydrazones, where O···O distances correlate with Hammett σ-values of the aryl substituents[94]. Other conjugated functional groups, such as those involving nitrogen (enaminones), should also exhibit this phenomenon. The authors suggest that the RAHB effect could have ramifications for the design of non-linear optical materials, since the hydrogen-bonded "resonant chains" have extensive electron delocalization and ground-state dipole moments[95].

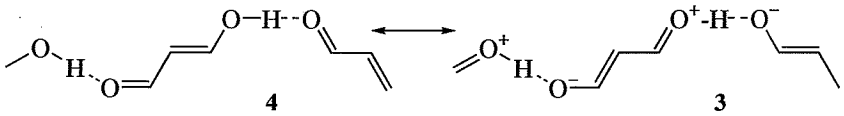

4 **3**

2.4 Packing Motifs of Carboxylic Acids and Primary Amides

Leiserowitz has extensively catalogued the motifs that carboxylic acids and amides are likely to adopt in crystals, and used symmetry, steric, and electrostatic arguments to rationalize these motifs. The broad outlines of his findings are as follows. Carboxylic acids "almost invariably" form cyclic hydrogen-bonded dimers[98]. While in principle a catermeric motif could form from either the *anti*planar (**5**) or the *syn*planar (**6**) COOH conformers, Leiserowitz found no examples of the former. Several examples of the latter are however known. The scarcity of the catermeric motif can be ascribed to either O···O repulsion, or weak distored hydrogen bonds resulting from the steric

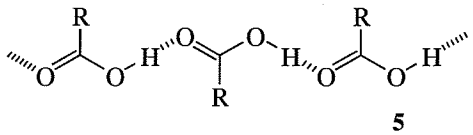

5

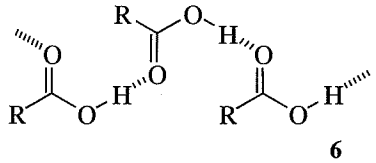

6

repulsion of the R groups. The only way in which carboxylic acids are observed to form hydorgen-bonded chains is if the molecule is a dicarboxylic acid. If one of the carboxylic acid groups is replaced with a primary amide, then there are two options for chain formation: one with acid–acid and amide–amide rings (homodimers, **7**) and one with acid–amide rings (heterodimers, **8**). In either chain, the second proton of the NH_2 group is unused in forming the chain and can link adjacent chains together. Consideration of the geometry of these layers of chains shows why the homodimer chains are not observed: optimal interchain hydrogen bonds would lead to electrostatic repulsion between oxygen atoms on adjacent chains of this class.

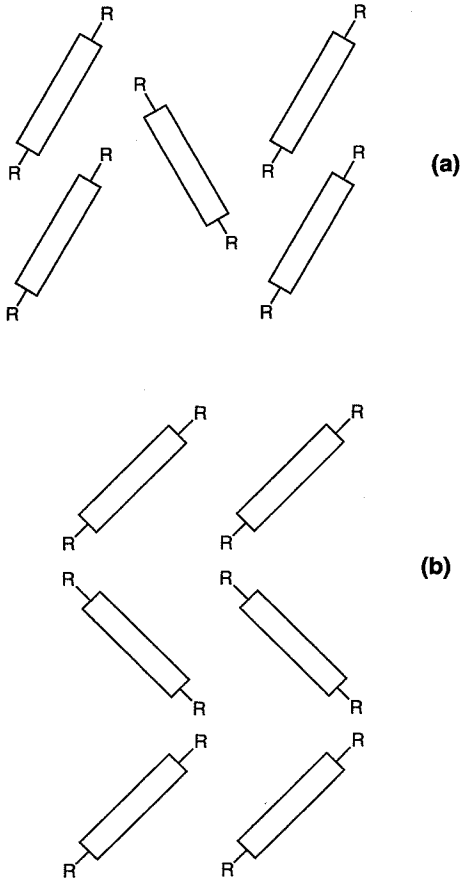

Figure 5.23 End-on views of hydrogen-bonded rods of primary amides in two possible packing arrangements. The top one, a herringbone motif, is observed, while the corrugated motif at the bottom is not.

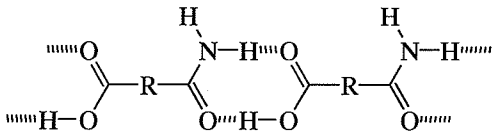

7

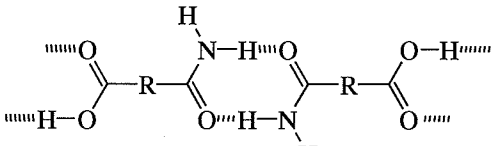

8

Similar issues are relevant to a consideration of the packing of primary amides[99]. Again, a ring structure similar to the carboxylic dimer, is overwhelmingly formed. Here, however, the *anti* amide protons that are external to the ring can be conveniently used to link rings into chains. Leiserowitz and Hagler apply symmetry operations to these chains to first generate two-dimensional layers, and then three-dimensional lattices. Only some of these possibilities are likely to be observed, because not all symmetry operations are consistent with the close packing of R groups and favorable interlayer electrostatic contacts. These arguments are able to rationalize, for example, why herringbone and not corrugated packing is observed (Figure 5.23). The authors suggest that a symmetry analysis of this sort could be used to construct a small number of possible packing arrangements that could then be evaluated by calculating the lattice energy (calculation of the lattice energy is discussed in Section 5).

3. SURVEY OF DESIGNS FOR CRYSTAL ENGINEERING

Recently, a number of innovative strategies that use hydorgen bonds to control crystalline structure have been explored[100]. Studies in this area focused deliberately on designing structures with specific shapes and sizes through non-covalent synthesis, and consequently led to the discovery of new structural principles and interesting topologies of packing. More importantly, these systems all used various elements of design to control the spacing and arrangement of structural units in the crystal. These elements of design provide chemists with a variety of choices for linking molecules together in an effort to design new crystalline systems. We will discuss each of these elements—charged and uncharged hydrogen bonds, rigid and flexible components, aliphatic and aromatic units—with respect to a given molecular system in the sections that follow.

3.1 Tubulands from Alicyclic Diols

Bishop and Dance discovered that alicyclic diols of varying ring size will self-assemble to give isostructural crystalline lattices[101–106]. The key structural features of these crystals are trigonal hydrogen-bonded "spines" interspersed with parallel channels (Figure 5.24). As a result of these channels, inclusion of molecules of solvent or other guests usually occurs. By controlling the shapes of the components of the host lattice, a range of topologies and diameters can be attained within the channel. More interestingly, the structure of the host lattice can be controlled by the geometrical and chemical structure of the included guest. In some cases, empty host lattices are also observed[106] (a characteristic that is unusual for organic hosts)[107]. One molecule of diol can be replaced in

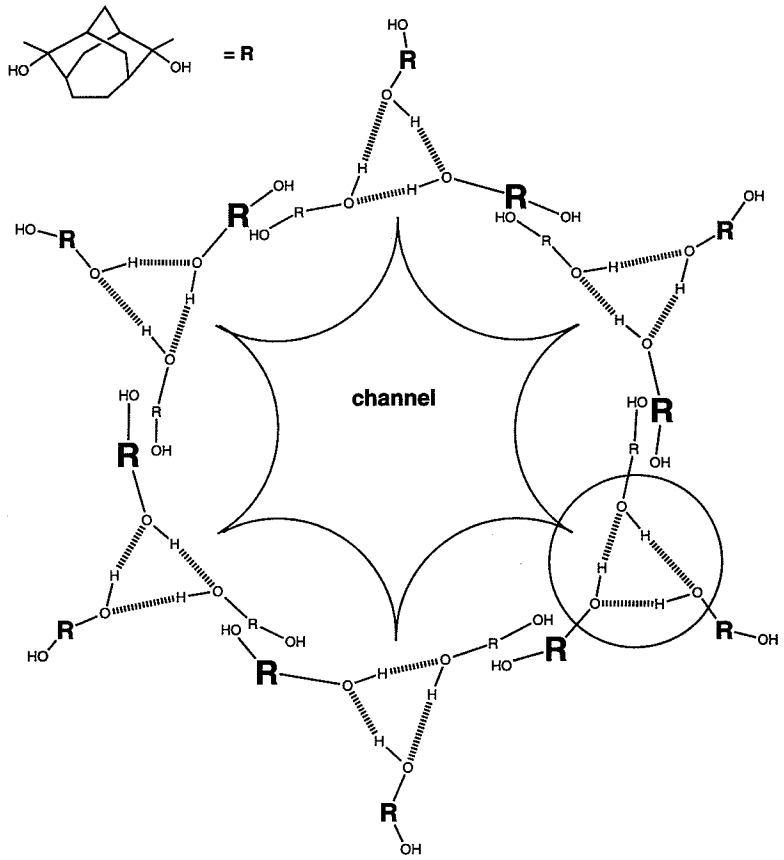

Figure 5.24 Schematic view of the packing of an alicyclic diol into the tubuland lattice, looking down one of the channels for guest enclathration. A hydrogen-bonded trigonal spine is circled.

the lattice of the host by another molecule capable of hydrogen bonding (e.g. a phenol) to give cocrystals[104]. In this way, other sorts of intermolecular interactions, such as Cl···Cl contacts or different kinds of hydrogen bonds, can be introduced into the crystal. Bishop and Dance have proposed guidelines describing the molecular features that must be present to form trigonal spines[102].

3.2 Ionic Hydrogen-Bonded Layers

Aakeröy and Seddon used hydrogen-bonded ionic salts to create robust crystalline architecture in one and two dimensions[108]. They generated entire families of crystal structures using various organic cations complexed with either a phosphate[37], malate[109], tartrate[110,111], or carboxylate anion[112]. The members of these families were compared for structural regularities; graph-set notation was indispensable in classifying the hydrogen-bonded networks[110–112]. A common motif consisted of chains of anions held together by strong OH···O$^-$ interactions (Figure 5.25). These chains were further linked into layers or three-dimensional networks by other hydrogen bonds, including weaker NH···O interactions involving ammonium counterions. Using different cations generally did not change the motifs of the anions (one-dimensional chains, two-dimensional layers, and three-dimensional networks) except in crystals built from phosphates. One of the goals of these authors was to use the

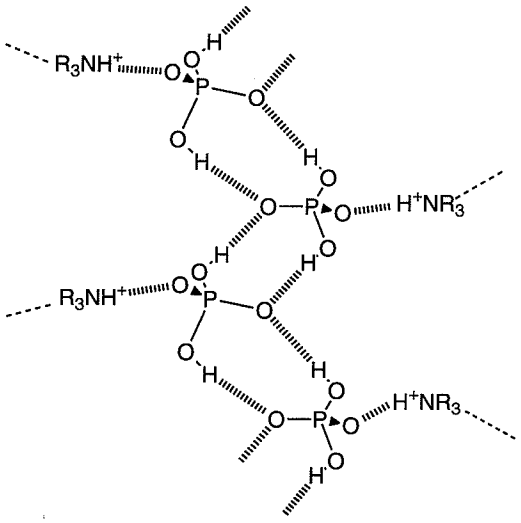

Figure 5.25 Chain of hydrogen-bonded anions (here, phosphate) of the sort used by Aakeröy and Seddon as "pattern generators". Protonation of a cocrystallized amine generates a counterion that can be used to link the phosphate chains into layers.

anions as "pattern generators"—that is, as reliable biulding blocks for crystal engineering—while using the cations to impart useful properties to the crystal[112]. For example, they hoped to use chiral components, either cations or anions, in conjunction with cations possessing a high degree of electron-delocalization to obtain materials that exhibit second-harmonic generation.

3.3 Conformational Control of Architecture: Chains and Helices

Hamilton found that bis(acylamino)pyridines cocrystallize with dicarboxylic acids to give 1:1 complexes that form extended chains (Figure 5.26)[113,114]. The crucial strategy for crystal engineering that these workers employed was to use components of complementary or mismatched sizes. When the two units were roughly equal in lengths, as in the case of 1,8-octanedicarboxylic acid and N,N′-bis[2-(6-methyl)pyridyl]-2,7-napthyldicarboxamide[114], both molecules were oriented approximately perpendicular to the ditrection of propagation of the hydrogen-bonded chain (Figure 5.27). When one component was substantially longer than the other (e.g. when 1,12-dodecanedicarboxylic acid is used)[114] a "slippage" of the molecules occurred that gave more acute tilt angles between the two components within the chain (Figure 5.27). By simply changing the size of either component, the width of the chains and the spacing of groups along the chains (e.g. the methyl groups or some other substituent on the pyridyl components) could be controlled reliably.

Control over the structure of the chains depended significantly on the conformtion of the acylamino moieties: the two acylamino groups had to adopt an *anti* orientation with respect to one another in order to form extended chains

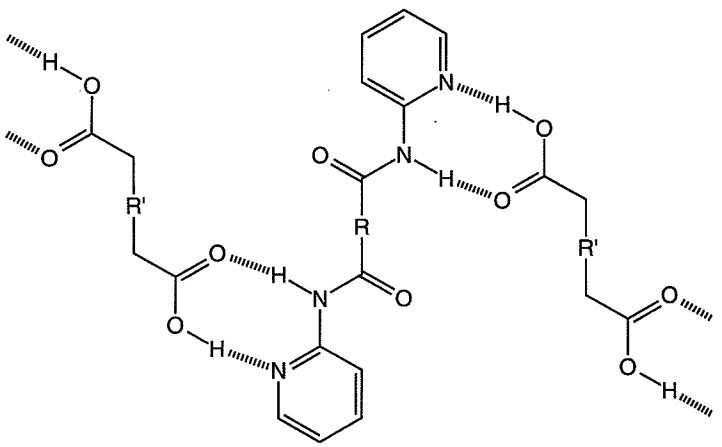

Figure 5.26 Hydrogen-bonded chains of bis(acylamino)pyridines and dicarboxylic acids.

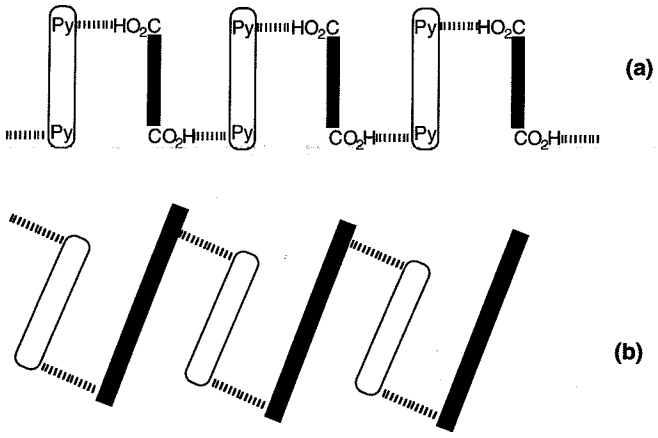

Figure 5.27 Schematic diagram showing the importance of matching the sizes of the two hydrogen-bonded components. (a) When they are approximately the same length, the molecular units are roughly perpendicular to the direction of the chain. (b) When one component is significantly longer than the other, both molecules tilt with respect to the chain axis.

(Figure 5.26). Adopting a *syn* orientation presented a convergent binding pocket that gave a closed dimeric complex[113,115]. When the acylamino groups were substituted *meta* with respect to one another on the aromatic ring, however, the *syn* conformation formed a binding pocket that was selective for only small

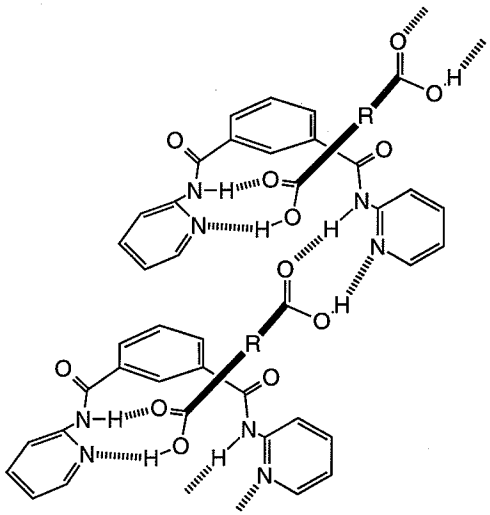

Figure 5.28 Hydrogen-bonded helix constructed from aminopyridine units linked to an isophthalate spacer and a dicarboxylic acid.

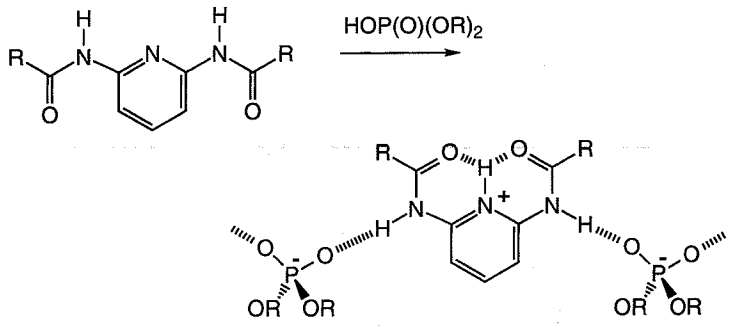

Figure 5.29 A conformational "switch". Protonation of the pyridine nitrogen swings the acylamino groups around to form intramolecular hydrogen bonds, and positions the NH groups to form intermolecular hydrogen bonds that form chains.

dicarboxylic acids. A mismatch in size between larger dicarboxylic acids and this pocket forced the acid to twist out of the plane of the bisacylaminopyridine to form a helical structure (Figure 5.28)[115]. Closest packing was achieved when helices of opposite handedness intercalated with one another. Aromatic stacking interactions appeared to be important in favoring this mode of packing. One drawback in controlling the formation of helical substructures was the occurrence of polymorphism. In one case, both a helix and an extended chain were observed[113].

Hamilton also reported preliminary work in controlling the *syn/anti* conformation by changing the state of protonation at selected sites[116]. When the pyridine ring of a 2,6-diamidopyridine was protonated, the two carbonyl oxygens pointed inward and formed a hydrogen bond with the pyridinium NH group (Figure 5.29). The formation of this complex forced the two NH group into an exo conformation, where they formed hydrogen-bonded chains with counterions such as a diarylphosphate.

3.4 One- and Two-Dimensional Aggregates Predicted Using Analyses of Symmetry

Fowler and Lauher used analyses of symmetry to predict and control the ways in which one-dimensional hydrogen-bonded assemblies aggreated into two-dimensional layers[117,118]. Their guiding principle is that "all intermolecular interactions between molecules of different asymmetric units will correspond to a specific symmetry operation:" a rule set by the symmetry of the lattice[118]. Hence the symmetry of a one-dimensional aggregate (which the authors call a rod group) can be combined with another symmetry operation to predict the symmetry of the resulting two-dimensional aggregate (which the authors call a layer group). These authors demonstrate that a maximum of 15 layer groups can

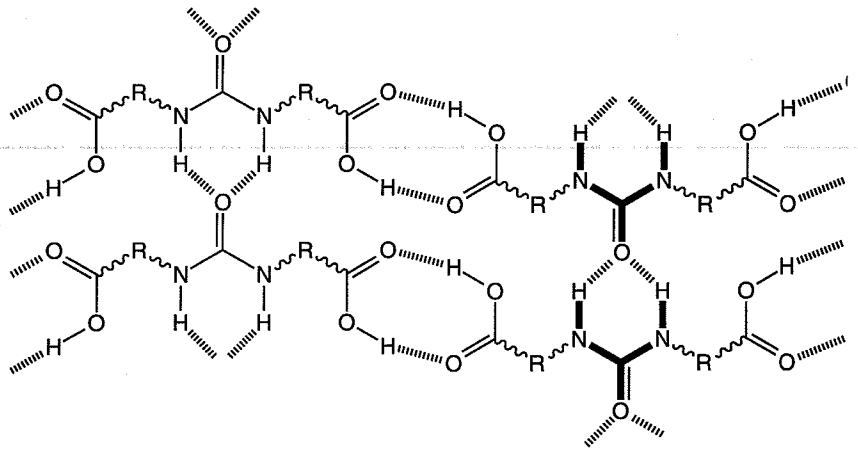

Figure 5.30 Layered motif of ureylene-dicarboxylic acids, with urea columns (bold) held together by carboxylic acid dimers.

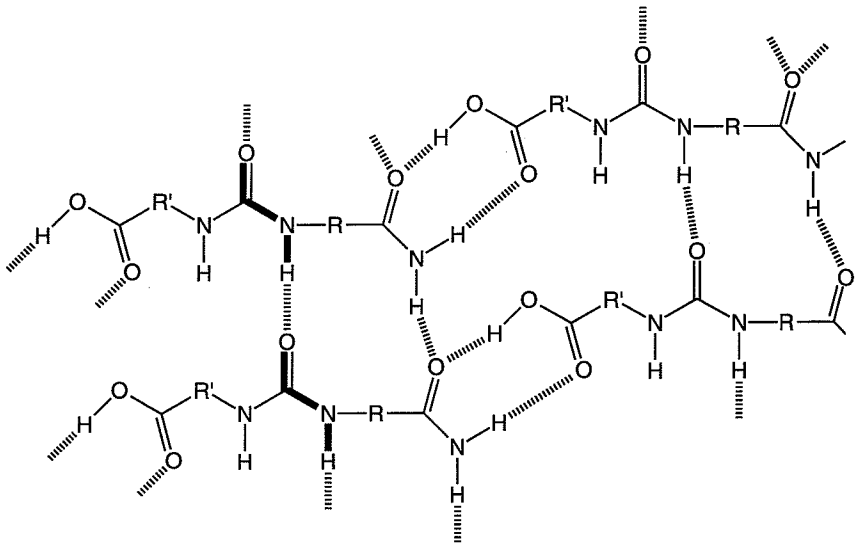

Figure 5.31 Non-equivalent terminal groups (here an acid and an amide) can lead to disruption of the familiar urea columns to give a different kind of urea chain (bold), again held together by acid–amide heterodimers.

form because some symmetry operations are inconsistent with the demands of closest packing in the crystal.

From a chemical standpoint, this scheme requires one motif of hydrogen bonds to generate the rod group, and another to tie the rods together into a layer. Fowler and Lauther's conceptual starting point was the chain motif formed by

ureas. Using N,N′-distributed ureas with carboxylic acids or primary amides as the substituents, they usually obtained rods crosslinked by chains of carboxylic acids (Figure 5.30)[118,119]. When the trwo substituent groups were not equivalent, however, unexpected patterns of hydrogen bonds occurred (for example, Figure 5.31). One strategy used by the authors to simplify the analysis of symmetries was to incorporate a chiral substituent into the urea, since there were fewer symmetry operations that could be used to pack chiral molecules[118].

Lauher and Fowler also expanded the skeleton of the urea by replacing it with an aminopyridone[120]. This replacement gave a rod motif similar to that of ureas, but increased the spcing between the rods from 4.6 Å to 6.7 Å. As with ureas, introducing additional hydrogen-bonding group to the ring of the pyridone promoted linking of the rods into layers. The most elegant of these designs used a nitrile to form a hydrogen bond to the *syn*-NH_2 proton, the one that is not used in the motif to build rods (Figure 5.32).

3.5 Open Lattices Constructed from "Tectons"

Wuest *et al.* used pyridones attached to rigid, linear, or tetrahedral cores (tectones, **9**) to assemble a range of lattice sizes and shapes.They have used these tectons as part of a supramolecular "building kit" to design zeolite-like

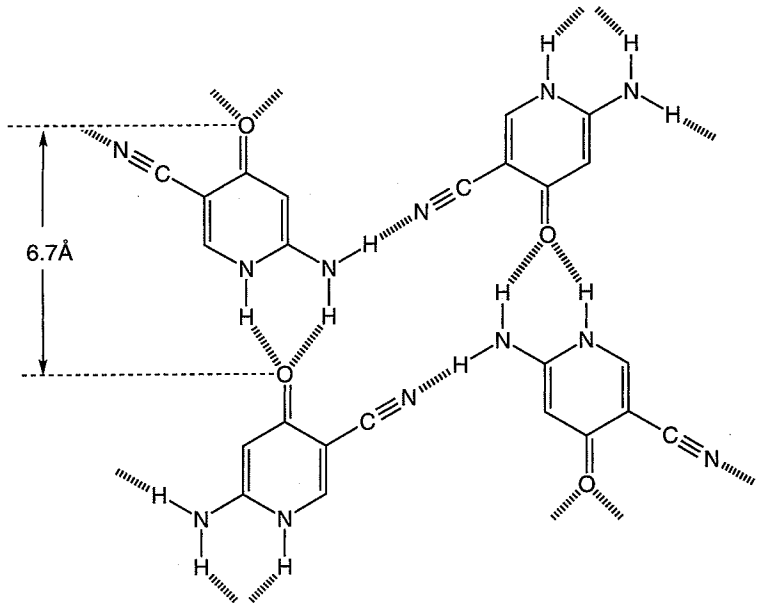

Figure 5.32 Incorporation of a vinylogous urea into a heterocycle leads to one-dimensional hydrogen-bonded rods than can again be joined into layers with an extra hydrogen-bonding moiety, here a nitrile.

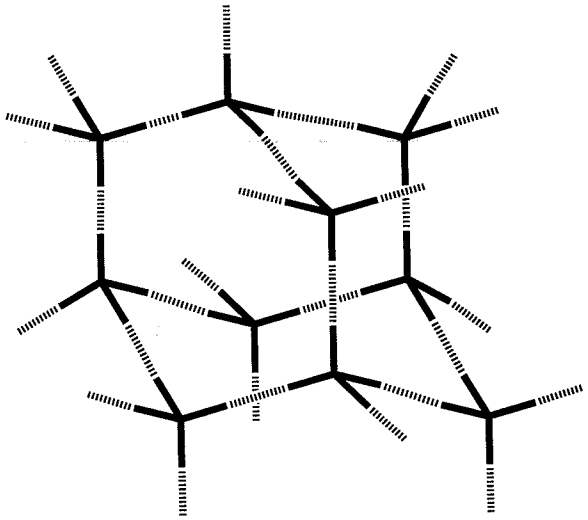

Figure 5.33 Schematic view of a diamondoid lattice obtained by self-assembly of a tetrahedral hydrogen-bonding molecule.

cages and diamondoid lattices in organic crystals (Figure 5.33). By changing the tetrahedral core from $C(C_6H_4C_2)_4$ to the analogous compounds of Si or Sn, channels with different volumes, or microporosities, could be engineered[121,122]. Different guests (usually carboxylic acids) were enclathrated with stoichiometries ranging from one molecule of valeric acid to four molecules of acetic acid per tecton. These cages did not form unless a guest of the proper size and shape to match the incipient channels was present. Moreover, when the size of the guest did not fit the channel, the tectons formed hydrogen bonds with the carboxylic acids[121,122].

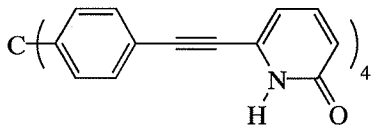

9

These authors also used rigid acetylenic units to link dipyridones together[123]. Depending on the site at which the C2 unit was joined to the pyridone ring, self-complementary dimers or open-ended chains resulted (Figure 5.34). An attempt at designing a cyclic trimer using this strategy was, however, unsuccessful, as competition with DMSO (as the solvent) during crystallization yielded an open-chain form[122]. Attempts to design structures based on dipyridones with flexible linkers were unsuccessful due to competition between intra- and intermolecular hydrogen bonding between the pyridone units[124].

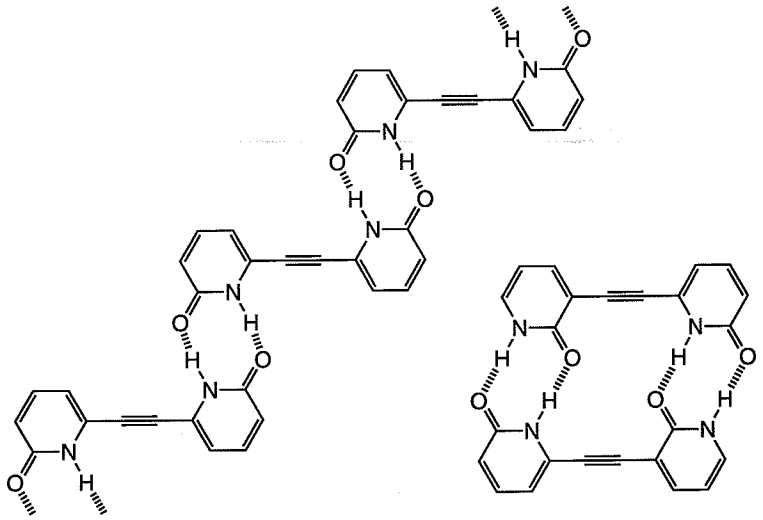

Figure 5.34 Two isomers of pyridones linked by an acetylene spacer can hydrogen bond to form a self-complementary dimer or an open-ended chain.

3.6 Layered Materials from Guanidinium Sulfonates

Etter and Ward have investigated salts formed from alkane- or arenesulfonates and guanidine for structural regularities that can be used in crystal design[125]. They predicted that the complementarity in shape and size of the three-fold symmetric ions—planar $C(NH_2)_{3+}$ and tetrahedral RSO_{3-}—would lead them to pair up into hydrogen-bonded dimers (Figure 5.35). In all 15 cases examined, dimers do form and are in turn linked into ribbons. They predicted that these ribbons would also aggregate into layers, which was in fact observed in 11 of these structures. These layers are not perfectly flat, but have variablility in the value of the inter ribbon angle. Three of the cases, for example, have inter ribbon angles less than 90°; the layers are formally present but are highly corrugated. In one structure (*para*-carboxyphenyl) layers are not formed at all. The authors rationalize these differences in planarity of the layers on the basis of the hydrogen-bonding ability of the alkene or arene substituents. Groups that hydrogen bond well, such as NO_2, OH, and COOH, compete with the guanidinium and sulfonate groups, and distort the inter-ribbon hydrogn bonds.

Another structural rationalization relates the size of the substituents to the kind of layer motif adopted. A bilayer structure, where two guanidinium sulfonate layers are stacked directly on top of each other and the substituents interdigitate with each other in a hydrophobic region, is formed if the substitutents are small (Figure 5.36). When the substituents are large, close packing of the hydrophobic groups cannot be achieved by this same kind of

Figure 5.35 Etter and Ward's design for layered materials: guanidinium cations and sulfonate anions can hydrogen bond to form dimers, which in turn can link up into ribbons and sheets. The ribbons that form sheets do not need to be coplanar, so there is an inter-ribbon angle θ that depends on the steric and hydrogen-bonding properties of the sulfonate R group.

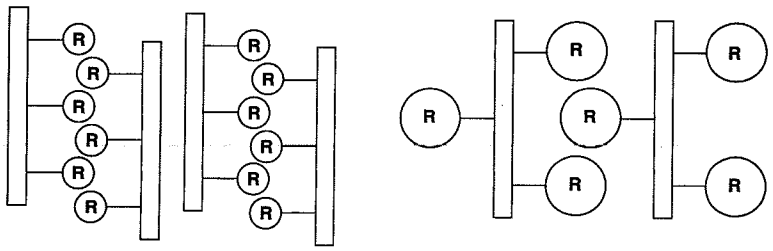

Figure 5.36 Two packing motifs for guanidinium sulfonate layers: (a) small substituents can interdigitate to give a bilayer arrangement; (b) larger substituents can only pack as single layers if close packing of the alkyl or aryl groups is to be achieved. The rectangles represent end-on views of idealized, perfectly planar hydrogen-bonded guanidinium sulfonate layers.

interdigitation, so a single-layer motif, with substituents alternating on opposite sides of the hydrogen-bonded layer, is formed. The authors hope to expand upon thse initial designs to build acentric materials: they speculate that the hydorgen-bonded layers could screen dipole–dipole interactions that lead to centrosymmetric packing by Coulomb interactions.

3.7 Layered Cocrystals Incorporating Urea Columns

Hollingsworth's group has applied spectroscopic methods to inclusion compounds of α,ω-disubstituted alkane guests in urea host lattices to obtain fundamental thermodynamic information about weak intermolecular interactions such as methyl/nitrile contacts[126,127]. While most of their work is outside the scope of this review, in the course of their studies on dinitriles they discovered that hydrogen bonds can form between the nitrile groups and the urea *syn*-NH protons[128–130]. The interesting structural feature is that there is a sudden change in the type of packing adopted depending on the length of the methylene chain. For 1:1 complexes of urea with $NC(CH_2)_nCN$ where $n = 3–5$, the NH···NC contacts link columns of urea molecules with rows of extended dinitriles to form layers (Figure 5.37)[128]. Longer guests, however, pack as inclusion complexes, either commensurate or incommensurate. The authors have performed lattice energy calculations and considered close-packing arguments to show that the switch in packing with length is due to the inherently poor packing of the methylene chains in the 1:1 layered complexes. As the number of CH_2 groups increases, the gain in van der Waals energy due to better chain packing in the inclusion compounds outweighs the cost of losing NH···NC hydrogen bonds (which appear to be less extensive in the channel-type inclusion compounds) from the layered motif.

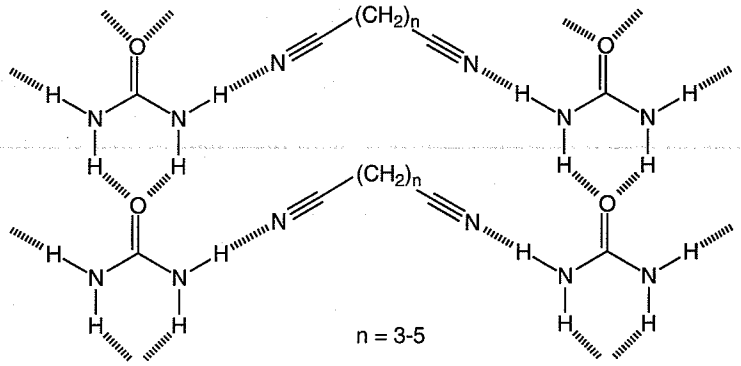

Figure 5.37 Layered packing of 1:1 complexes of short dinitriles with urea. The methylene chains are not in van der Waals contact with each other.

In terms of crystal engineering, Hollingsworth's group developed a clever way to circumvent this switch in packing motif, which occurs with longer guests: Their solution was to add hydrogen-bonding capacity at the middle of the methylene chain, so that 1:1 layer packing would not be energetically disfavored relative to inclusion-type packing[128]. The moiety that they incorporated was another urea group (Figure 5.38). The methylene chains are still not closely packed, but the added hydrogen-bonding interaction makes up for this situation. The resulting structure is thus reminiscent of Fowler and Lauher's layered structures[120], except that while one urea column is covalently a part of the crystal, the other column is held in place by intermolecular NH···NC interactions.

In addition, Hollingsworth *et al.* have expanded upon a statistical study of packing efficiency by Gavezzotti, who had demonstrated a correlation between

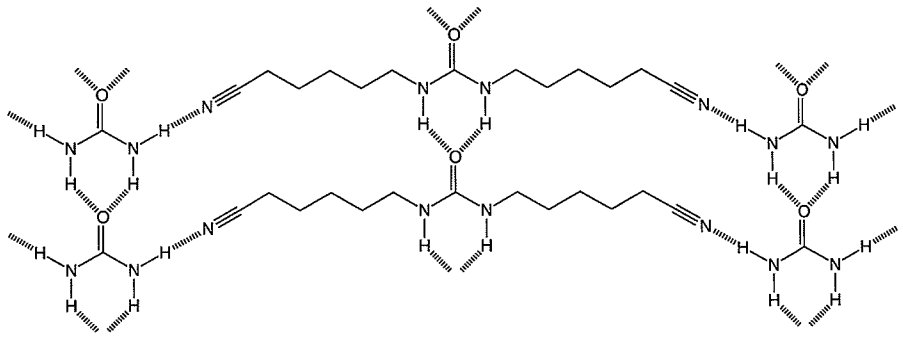

Figure 5.38 The incorporation of hydrogen-bonding functionality (here a urea group) in the middle of a long-chain dinitrile allows formation of a 1:1 layered complex with urea instead of a switch to a channel-type inclusion compound.

the average electron density of a crystal (in units of e/Å^3) and average atomic number of the unit cell[131–133]. Gavezzotti's study did not include data from hydrogen-bonded crystals, and Hollingsworth has now explicitly done so[128]. The result shows that there is no intrinsic need for hydrogen-bonded crystals to pack with decreased efficiency—that is, with open lattices that scarifice close packing for a greater number of hydrogen bonds. This correlation also explains the switch from 1:1 layered cocrystals to inclusion compounds in the dinitrile system under investigation: the hypothetical electron density value for the unobserved layer-type complex with $NC(CH_2)_6CN$ is very low, while that for the observed inclusion compound is in good agreement with the statistical trend. Calculations of this sort could also be useful for rationalizing an abrupt change in packing motif in other families of structural homologues.

3.8 Diamondoid Networks

Zaworotko's group succeeded in designing microporous materials using metal carbonyl clusters of $[M(CO)_3(m_3\text{-}OH)]_4$, (where M = Mn or Re) as building blocks (**10**)[134–136]. In these clusters, the bridging OH groups were oriented tetrahedrally; therefore cocrystallization with hydrogen-bond acceptors as spacer units gave diamondoid lattices that interpenetrated to different degrees, usually 2-fold or 4-fold (Figure 5.39). The tetrahedral geometry of the OH groups gave structures that were two-dimensional: they gave a "doubly interwoven carpet-like structure". Spacers used by Zaworotko included diamines, hexamethylenetetramine, and 4,4′-dipyridine, which formed OH···N hydrogen bonds; and toluene or naphthalene, which formed OH···arene hydrogen bonds[134]. Three-component networks, where hydrogen bonds with alcohols link the metal clusters and 4,4′-dipyridine, have also been formed[135]. These structures, however, were two-dimensional, also giving a "doubly interwoven carpet-like structure". Zaworotko controlled the size of the micropores in these lattices by changing the length of the spacer to enclathrate different molecules of solvent selectively.

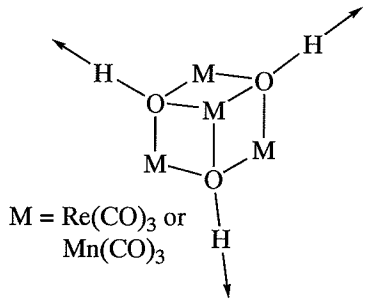

10

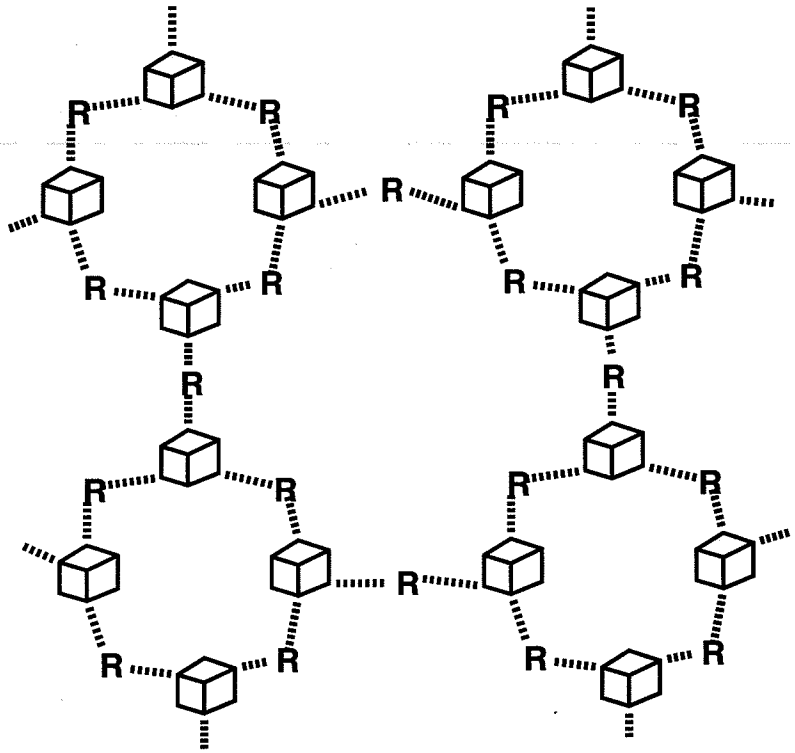

Figure 5.39 Schematic view of a two-dimensional fragment of a diamondoid lattice, where the cubes represent $M(CO)_3(OH)_4$ clusters and the spacers R could be diamines, bis-phosphine oxides, or aromatic hydrocarbons. Interpenetration of two-dimensional layers through the central pore can lead to construction of the three-dimensional lattices.

In another study, Zaworotko replaced the terahedral metal cluster with a functionally-equivalent tetraprotonated cyclam as a proton donor to form the network[137,138]. The counterions ranged from chloride and trifluoroacetate to ferrocenedicaboxylate, all of which bridged neighboring cyclams using charged hydrogen bonds. Zaworotko has also obtained two-dimensional networks with microchannels for solvent with these components. These results demonstrate the versatility of Zaworotko's approach to controlling microporosity by interchanging tectons with different geometries.

4. DESIGNS BASED ON CYANURIC ACIDS AND MELAMINES (THE CA • M LATTICE)

Our strategy has focused on controlling the various motifs present in the 1:1 complex between cyanuric acid and melamine (CA • M) shown in Scheme 5.2.

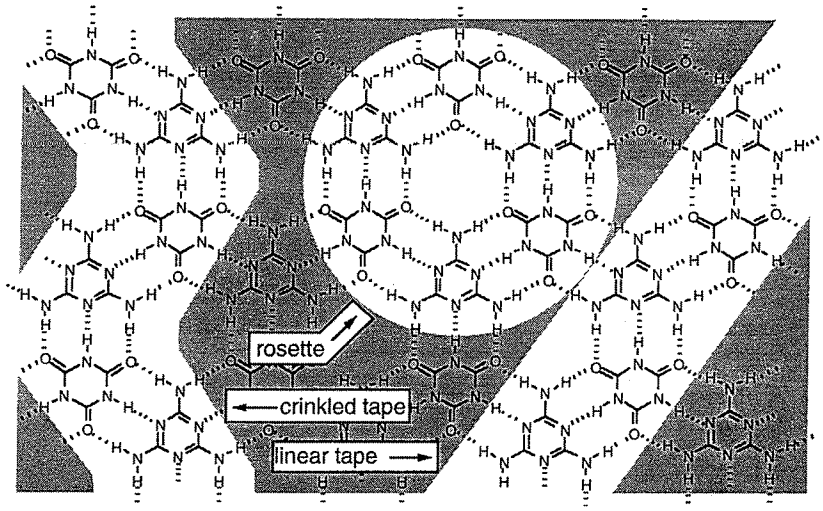

Scheme 5.2 Schematic view of the cyanuric acid and melamine (CA • M) substructures: linear tape; crinkled tape; and rosette.

We and others believe the structure of CA • M consists of infinite hydrogen-bonded sheets[139]. A report has also appeared in the literature describing the crystal structure of a 1:1 complex of cyanuric acid with melamine, although it consists of solvated, protonated dimers and not a layer structure, since it was crystallized from 3 M HCl[140]. Although no crystal structure is available for CA, data from X-ray powder diffraction (XPD) are consistent with this structure: one of the strongest reflections gave a *d*-spacing of 3.4 Å, the expected value for interlayer separation[141].

We have used the group of three hydrogen bonds formed between the components of CA • M to construct linear, crinkled, and cyclic motifs in organic crystals (Scheme 5.2 and Figure 5.40)[142–146]. Linear and crinkled motifs are substructures that we refer to as "tapes"; cyclic motifs are referred to as "rosettes". Systems based on CA • M are attractive because the derivatives of the components are easy to synthesize, and thus a range of substituents or functional groups can be easily introduced. We used derivatives of cyanuric acid rather than barbiturates for their ease of synthesis and more convenient solubilities. Also from a paragmatic view, we have never been able to obtain diffraction-quality crystals of complexes incorporating derivatives of cyanuric acid. This failure is most likely due to the greater acidity of cyanurates[142], which leads to the formation of aggregates that are more insoluble than those based on barbituric acids. In addition to these solid-state structures, we have constructed a range of soluble aggregates basd on the cyclic motif[147].

Our goal was to determine what structural features of the molecules would allow us to control the formation of the linear, crinkled, and rosette motifs. We

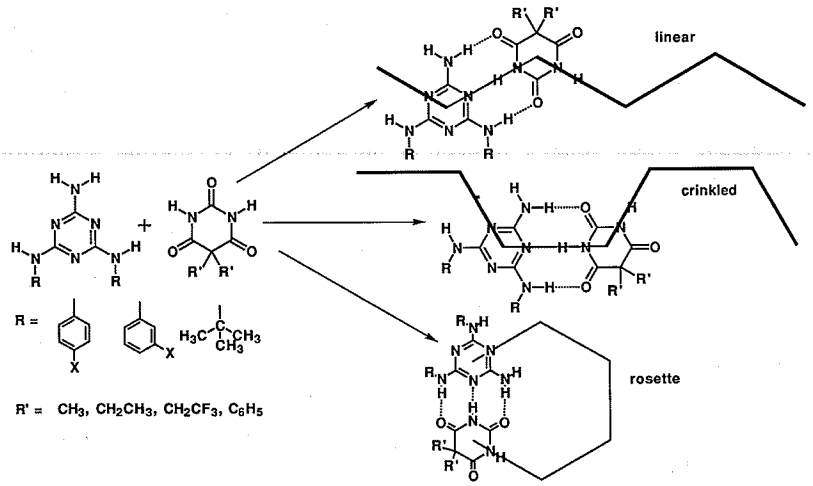

Figure 5.40 Schematic view of the proposed two-dimensional sheet of the complex between cyanuric acid and melamine (CA•M). Substructures are outlined: rosette; crinkled tape; and linear tape.

reasoned that blocking hydrogen bonding in some directions was a logical tactic that would promote the formation of a small number of crystalline substructures: these substructures are geometrically and conceptually simple; this simplicity aids in their classification.

Our experiments focused on structures of complxes between barbituric acids and three different classes of melamines:

- N,N′-bis(*para*-X-phenyl)melamine, where X = H, F, Cl, Br, I, CH_3, CF_3, CO_2Me, and $C(CH_3)_3$, cocrystallized with 5,5-diethylbarbituric acid (**11**)
- N,N′-bis(*tert*-butyl)melamine cocrystallized with 5,5-di-X-substituted barbituric acids, where X = CH_3, CH_2CH_3, CH_2CF_3, and C_6H_5 (**12**)
- N,N′-bis(*meta*-X-phenyl)melamine, where X = H, F, Cl, Br, I, CH_3 (**13**) CF_3, CO_2Me, and $C(CH_3)_3$, cocrystallized with 5,5-diethylbarbituric acid

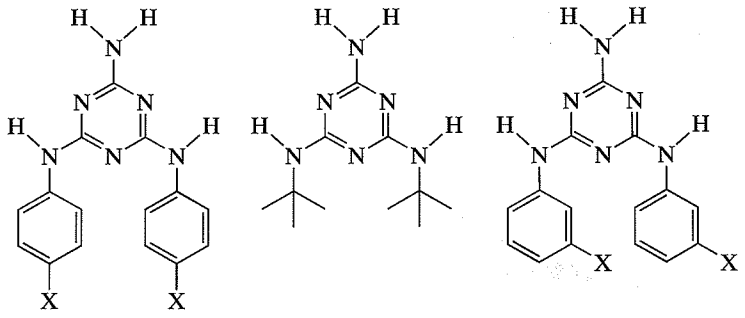

11 **12** **13**

The appproach we followed in designing these families is a familiar one in physical–organic chmistry, namely incremental variation in the size of substituents (X). Considering entire families of complexes is necessary if we are to discern trends in packing patterns and relate them to molecular structure. This strategy, which relates molecular structure to crystalline structure, is central to crystal engineering.

To facilitate analyses, we classified the substructures of the crystal into several hierarchical levels. These levels constitute a scheme that is intended to provide points of attack for purposes of design at these different levels: we hope to determine the molecular features responsible for these substructures, and then demonstrate that these features can be manipulated rationally to give the desired crystalline structure or property. The various levels of substructures are shown in Figure 5.41. The primary level of substructure is simply the identity, stoichiometry, sequence, and conformation of the constituent molecules. The secondary level consists of the motif produced by aggregation of the individual molecules—in this case, tapes. These tapes can be linear, crinkled, or perhaps a more complicated hybrid of both. The tertiary level is constructed in turn from these secondary levels. For example, we found that tapes can aggregate as dimers or as sheets. We expect that tapes should pack with their long axes parallel to each other in the crystal to maximize van der Waals contacts: as a

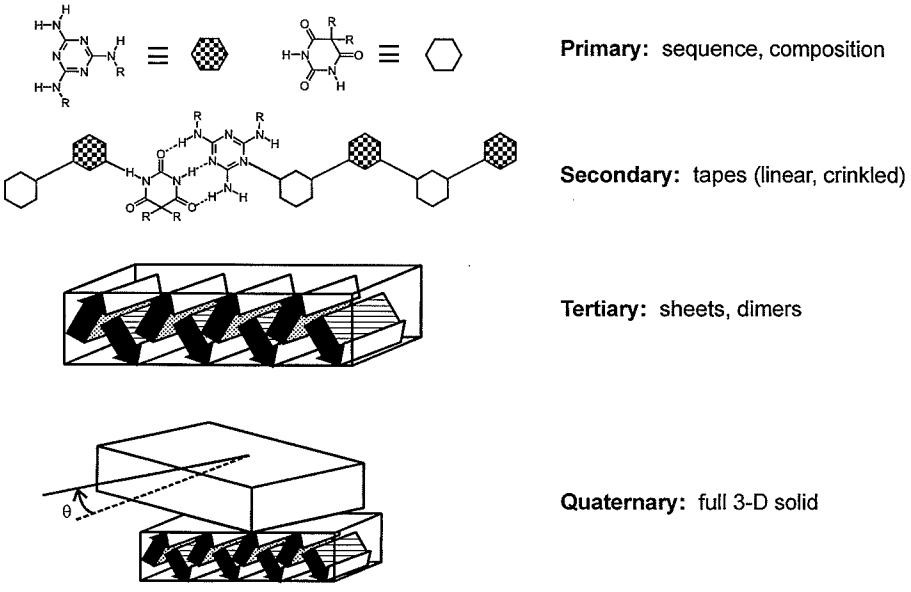

Figure 5.41 Hierarchical levels of crystalline architecture.

broad generalization, the ridges and grooves that tapes present along the surface of a sheet or dimer should pack snugly against each other to minimize empty space in the crystal. We also hypothesized that steric repulsion between adjacent melamines would be unavoidable at some point if we increased the size of the substituents on the phenyl rings of melamine: large substituents should not be able to pack in the linear motif.

The most important points we will stress in the discussion of our work are that:

- the CA • M lattice provides several robust structural motifs for the design of organic solids
- some motifs can be controlled by a choice of substituents
- the possibility for variations in molecular conformation complicates the interpretation of packing because of polymorphism

4.1 The *para*-substituted Diphenylmelamine Family

4.1.1 Linear Tapes

Cocrystals built from N,′-bis(*para*-X-phenyl)melamine, where X = H, F, Cl, Br, I, CH_3, CF_3, formed linear tapes (Figure 5.42)[142]. Figure 5.42 shows the structural features of these linear tapes from two different viewpoints. One important feature is that the substituents on melamine are separated from the ethyl groups of barbital on opposite sides of the tape. The backbone of these tapes is held together by three hydrogen bonds as in the CA • M lattice. Increasing the size of substituents on melamine from H to CF_3 did not interfere with the formation of these linear tapes. Reliability of this sort is essential for studies attempting to compare a range of substituents in the solid state: if a system adopts a fundamentally new motif with every change of substituent, then it would be useless for purposes of design unless each new motif could be predicted beforehand.

While the packing of each memeber of the *para*-family has interesting structural features, the *trends* in packing for this family are more instructive in developing guidelines for crystal engineering. One of the strengths of this cocrystalline system is that different types of substructures are identified easily.

4.1.2 Crinkled Tapes

We further reasoned that *para*-substituents larger than those that gave linear tapes would force the tape from linear to crinkled. The substituent that we used to test this hypothesis was the CO_2Me group. Figure 5.43 shows the crinkled tape obtained from a complex of N,N′-bis(4-methoxycarbonyl-phenyl)melamine with barbital[143]. In this structure, the CO_2Me groups are oriented

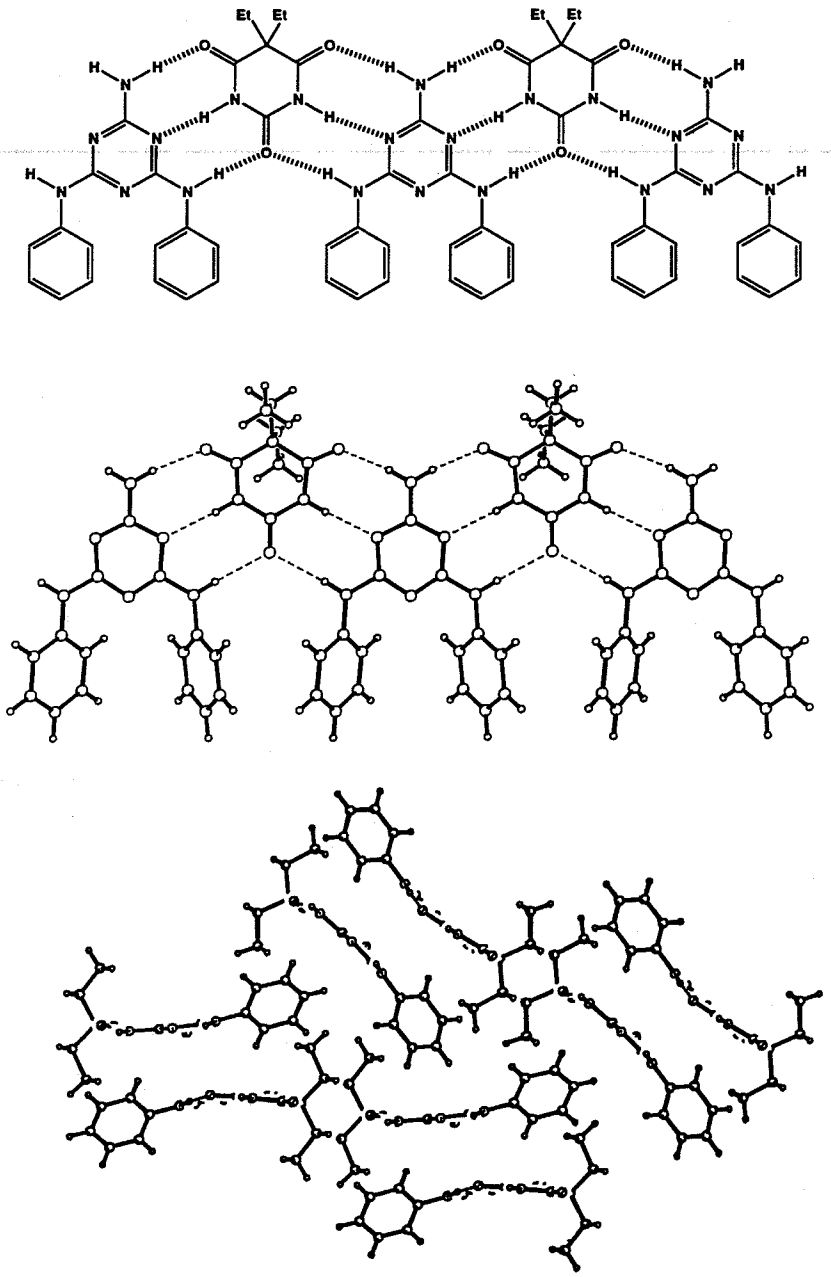

Figure 5.42 Two views of the crystal structure of the complex between N,N-diphenylmelamine and 5,5-diethylbarbituric acid. Middle: a view of the hydrogen-bonded linear tape from the top. Bottom: end-on views of the packing of the linear tapes, looking down their long axes.

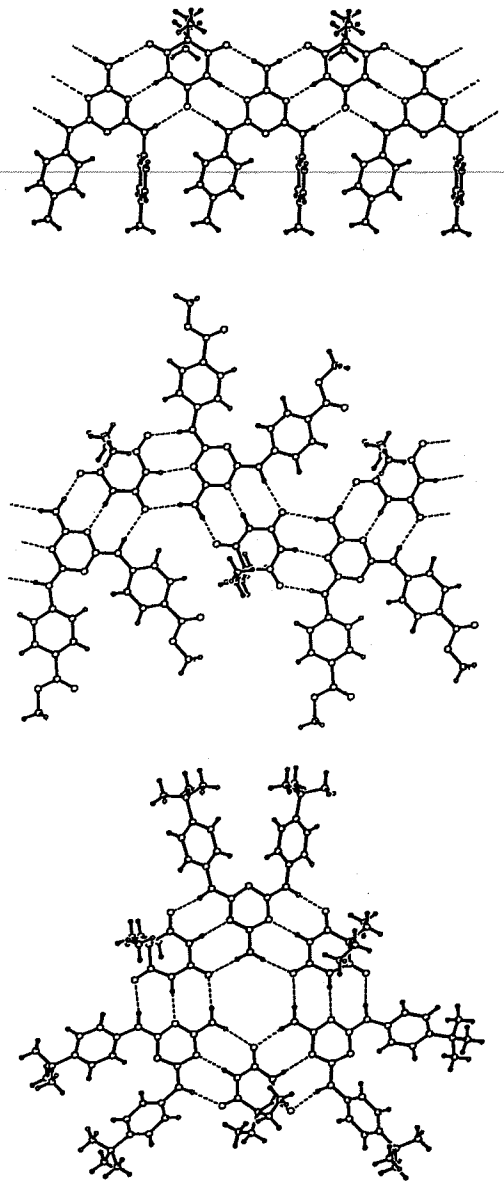

Figure 5.43 Three varieties of hydrogen-bonded complexes obtained from the CA • M system. Top: linear tape from N,N′-bis(*para*-methylphenyl)melamine and barbital. Middle: crinkled tape from N,N′-bis(*para*-carboxymethylphenyl)melamine and barbital. Bottom: rosette from N,N′-bis(*para*-t-butylphenyl)melamine and barbital.

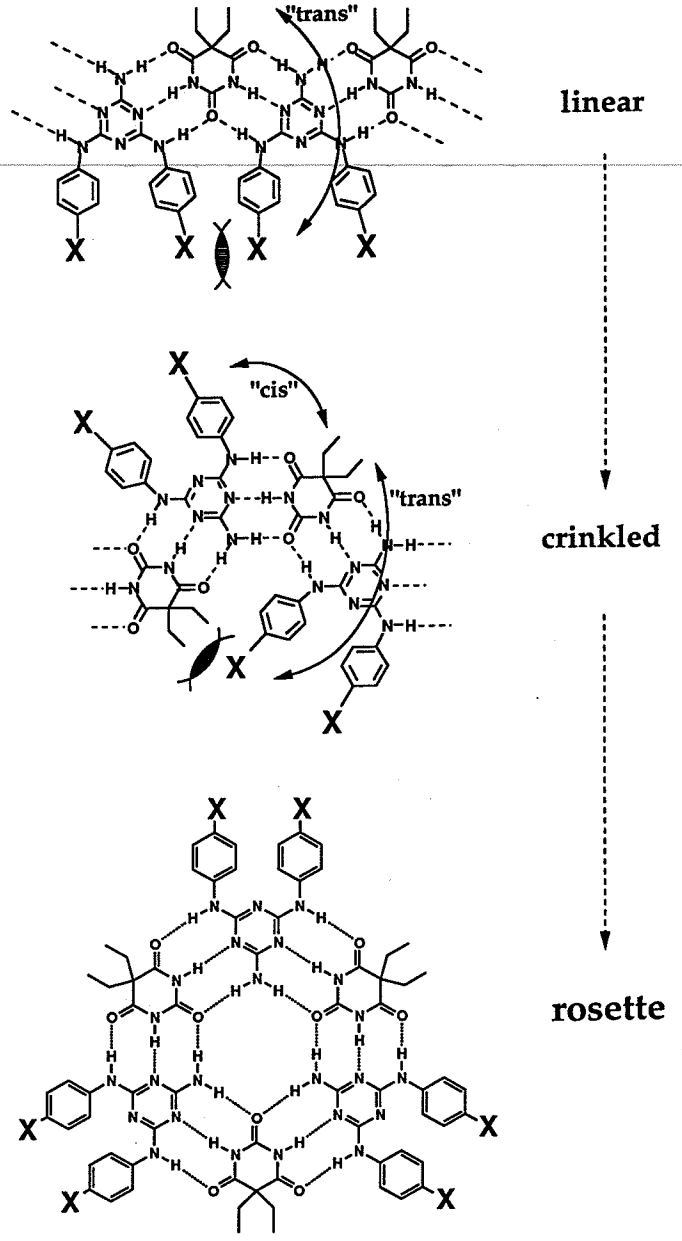

Figure 5.44 Steric repulsion between adjacent melamines leads to changes in the tape motif.

approximately coplanar with the hydrogen-bonded backbone of the tape, rather than pependicular to the backbone. The CO_2Me groups most likely adopted this coplanar orientation to pack efficiently at the tertiary level. This inference highlights an important aspect of crystalline structure, namely that there can be an interplay between the various forces of packing at different levels of substructure. In other words, the motif that is adopted at the secondary level—linear or crinkled—can depend on the packing at higher levels.

4.1.3 Rosettes

We sought to circumvent problems in predicting the packing of tapes with flexible substituents that have anisoptropic shapes (the CO_2Me group) by using those that are isotropic, and also to ensure that linear tapes could not be formed by using a substitutent of sufficient size. A *tert*-butyl group satisfies these requirements. The complex of N,N′-bis(*tert*-butylphenyl)melamine with barbital did not, however, adopt any of the tape motifs, but instead formed a cyclic hexamer, or rosette (Figure 5.43)[143]. We believe that this complex forms and packs as a rosette to permit maximal separation of the substituents from each other (Figure 5.44).

4.2 The Bis(t-butyl)melamine Family

4.2.1 Crinkled Tapes

The results from the *para*-substituted diphenylmelamine series suggest an upper limit in size for the groups attached to the melamines (that is, both the phenyl ring and its substituents) that can be accommodated and still maintain the crinkled motif; groups larger than this limit produce the rosette motif. With this observation in mind, we found that the crinkled motif could be maintained by replacing the phenyl rings of melamine with *tert*-butyl groups[144]. Four complexes built from N,N′-bis(*tert*-butyl)melamine with different barbiturates all crystallized in the crinkle motif (Figure 5.45).

These example illustrate the value of steric effects in controlling *secondary* substructure in the compounds of these crystals.

4.3 The Family of *meta*-Substituted Diphenylmelamines

We examined the crystal packing for N,N′-bis(*meta*-X-phenyl)melamines where X = H, F, Cl, Br, I, CH_3, and CF_3, cocrystallized with barbital (Figure 5.46) [145]. We wished to determine of moving substituents from the *para* position to the *meta* position would significantly alter the type of motif that formed during crystallization. We found that derivatives of melamine from this

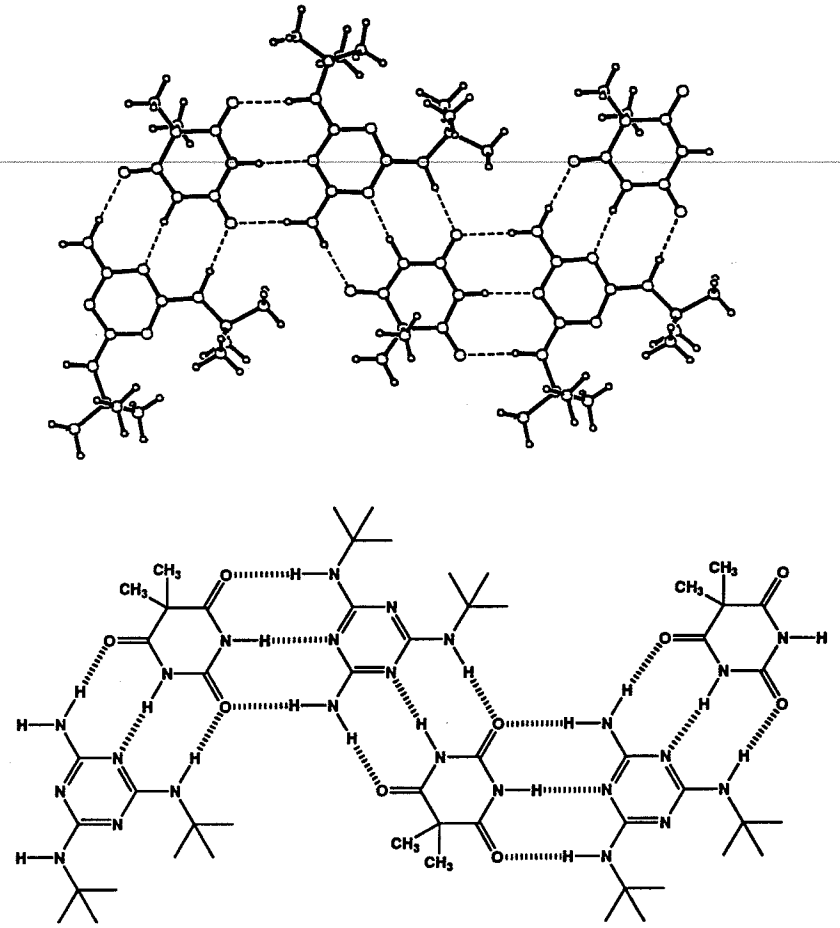

Figure 5.45 The crinkled tape obtained from di-*tert*-butylmelamine and 5,5-dimethylbarbituric acid.

meta-substituted series showed no correlation between the size of the substituents and the resulting packing motif. The complexes with the larger substituents CH_3, I, and CF_3 packed as linear tapes, while those with Br and Cl adopted the crinkled motif (Figure 5.46; none of these structures was checked for polymorphism). In the latter two cases, there was a contact between a phenyl hydrogen and a barbital oxygen across the bay region of the crinkled tape, which appeared to stabilize the crinkled motif.

A serious problem with the *meta*-family that hindered us from controlling structure was the high frequency with which molecules of solvent were trapped in the crystalline lattice. We believe that the propensity for molecules of solvent

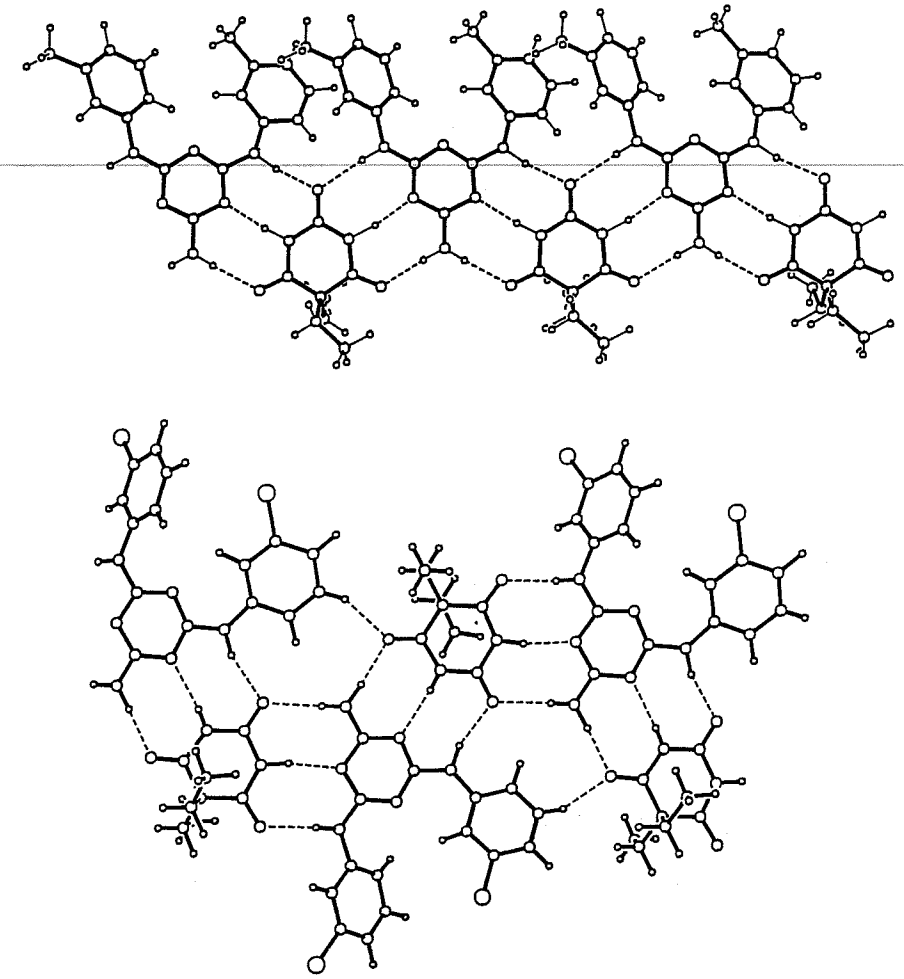

Figure 5.46 Two tapes from the *meta*-family. Top: linear tape from N,N′-bis(*meta*-methylphenyl)melamine and barbital. Bottom: crinkled tape from N,N′-bis(*meta*-chlorophenyl)melamine and barbital, showing intra-tape CH···O contacts.

to be incorporated into the lattice of these *meta*-substituted diphenylmelamines reflect the fact that they do not pack efficiently.

4.4 Polymorphism

Studies in crystal engineering are incomplete without searching for the occurrence of polymorphism, because organic molecules often can pack in

isoenergetic, or nearly isoenergetic arrangements[10–15]. Moreover, anticipating whether a given series of molecule will be prone to polymorphism is difficult, because so many factors can affect packing. One of our goals has been to find robust systems that limit the possibility of polymorphism. There are several experimental methods that can be conveniently used to search for and characterize polymorphs: X-ray powder diffraction[148,149], and solid-state NMR spectroscopy are especially useful[150–152]; thermochemistry is also very useful, but substantially more difficult experimentally.

We tried to induce polymorphism by crystallizing members of the *para*-series from a variety of different solvents[153]. All but two complexes gave just one crystalline form. It is important to stress, however, that we crystallized these complexes under a limited range of conditions: we did not vary temperature or control the rate of evaporation.

Attempts to obtain single crystals of polymorphs were successful for N,N′-bis(*p*-Br-phenyl)melamine•barbital, and unsuccessful for N,N′-bis(*p*-CF_3-phenyl)melamine•barbital[153]. A comparison of the packing of the two Br polymorphs (based on single-crystal diffraction) show that one packs isomorphously to the Cl complex, while the other packs similarly to the I and CH_3 complexes (Figure 5.47). Since bromine is intermediate in size for the substituents in the *para* series (H to CF_3), melamines with this substituent appear to have access to the packing arrangement associated with either smaller or larger substituents.

4.5 Strengths and Weaknesses of the CA • M System

The CA • M lattice represents a useful starting point for crystal engineering because it predictably forms hydrogen-bonded substructures: tapes or rosettes. These motifs are generated reliably: the triplet of hydrogen bonds that holds the components together are strong enough so that they are not easily disrupted. We have not, however, succeeded in introducing polar peripheral substituents, where strong polar interactions may disrupt these motifs. We have developed a model for crystal engineering based on the hierarchical packing of substructures in this system that permits limited studies of packing in crystals. We were also able to rationalize each level of packing by identifying the molecular features responsible for promoting each substructural motif. Our clearest success has come in rationalizing general trends in secondary architecture in complexes with *para*-substituted diphenylmelamines[143]. By altering the size of the substituents, we were able to control whether the molecules adopted a linear tape, a crinkled tape, or a rosette motif[143,154].

Despite these virtues, the number of families of complexes based on the CA • M lattice that comply with this scheme of analysis and design, and the potential of this system in crystal engineering, may be limited. Several features of this system contribute to these limitations. First, growing diffraction-quality

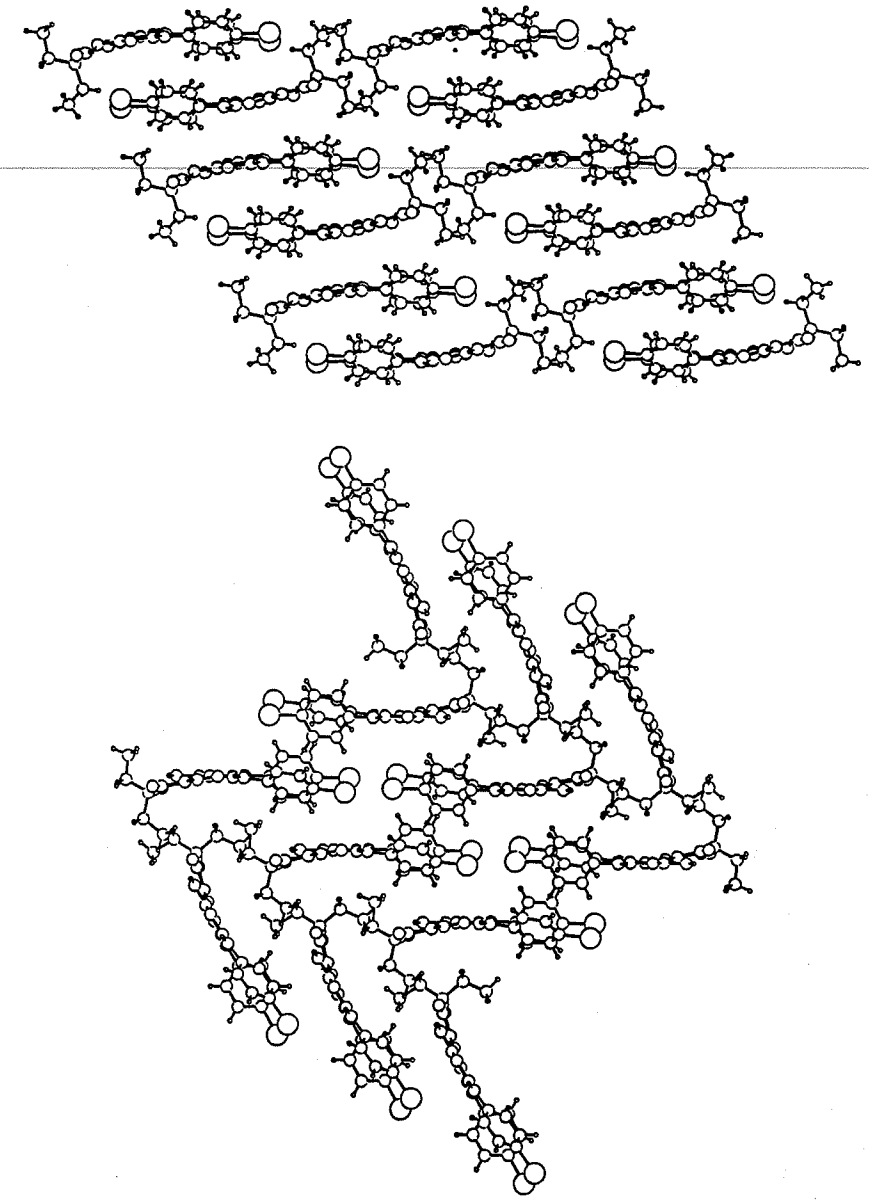

Figure 5.47 End-on packing views of linear tapes for two polymorphs of the complex between N,N′-bis(*para*-bromophenyl)melamine and barbital. The top polymorph packs isomorphously to the *para*-chloro complex, while the bottom polymorph packs similarly to the *para*-iodo and *para*-methyl complexes.

crystals in this series remains slow and difficult; for an ideal system, crystallization would be straightforward. Second, the system does not tolerate polar substituents well. Third, the presence of polymorphism decreases the level of control that can be exercised in the system: complexities in packing due to conformational isomerism may be one of the biggest hurdles hindering the rational design of molecular crystals. In principle, each accessible conformation can pack as a separate crystalline phase. Polymorphism of this sort occurs both occasionally in the *para*-family (where it is associated with size of substituents) and in the *meta*-family. In both series, the ethyl groups of the diethylbarbital can also contribute to conformational polymorphism. Presently, we cannot predict the packing of these tapes at the tertiary level of substructures.

We are currently studying other model systems containing rigid molecules that form tapes[155]. The use of rigid molecules should limit the conformational isomerism we encountered in the CA • M system. While the CA • M system has many attractive characteristics, it is probably too complex to serve as a basis for extensive studies at the current state of development of the field.

5. COMPUTATIONAL APPROACHES TO PREDICTING THE STRUCTURE OF ORGANIC CRYSTALS

A number of new computational strategies have emerged that promise to be useful in crystal engineering. In this section, we will highlight these recent computational efforts that ultimately intend to *predict* the crystal structure of organic molecules using only information about the geometric structure of a single molecule. Other methods for predicting the crystalline structure of organic molecules existed before those reviewed here[156,157], but these earlier methods typically required either additional experimental information or the presence of a plausible hypothetical crystal structure[158], before an accurate prediction of the final crystal structure could be made. In other words, the methods excluded from this section are only appropriate if given much information about the crystalline environment.

The methods reviewed here rely on two important assumptions about the experimental crystal structures: that molecules of solvent do not affect the crystal structure, and that the arrangement of the molecules in the crystal represents the thermodynamic minimum in free energy. These assumptions are only valid for robust crystal systems—that is, for systems with a well-defined global minimum in free energy that do not form polymorphs. These methods also neglect entropy in their calculations. In the future, methods such as normal mode analyses[159,160], and molecular dynamics[161], which can estimate the vibrational entropy, may be useful in conjunction with these methods.

At the heart of the computational strategies to predict the packing of organic molecules we consider here is the calculation of the lattice energy (U_{latt} using

atom–atom potential functions*:

$$U_{\text{latt}} = \sum_{i,j}(E_{\text{vdw}} + E_{\text{elec}}) \quad (1)$$

In equation 1, the van der Waals (E_{vdw}) and electrostatic (E_{elec}) energies are summed between atoms i in a single molecule and atoms j in the other molecules included in the computation. The components in Equation 1 can vary, but they are empirical descriptions of the energy of the crystal[162]. The parameters in the components of Equation 1 are derived from experimental and quantum mechanical data; therefore, calculating U_{latt}, rather than relying on methods that use statistical correlations, represents the most physically meaningful way of evaluating crystal structures.

Currently, the most promising methods for predicting the crystalline state of organic molecules, based solely on the geometric structure of a single molecule, involve computing U_{latt} for the possible arrangements of rigid and semi-rigid molecules in the crystal[25,163]. There are, however, two significant limitations in computing U_{latt} of these arrangements. First, the very large number of spatial arrangements—based on translational and rotational changes—intrinsic to small organic molecules can render the calculations intractable†. A computer evaluates U_{latt} for each of these arrangements to find the lowest value, which is then assumed to represent the arrangement observed in reality. In addition, the possibility of conformational isomerism in most organic molecules substantially complicates the problem of rationalizing crystal structures by broadening the range of structures that has to be examined. Second, the accuracy of the force field used in the computations can limit the ability of the computations to differentiate between polymorphs (often different packing arrangements differing in energy by less than ~ 1 kcal/mol). (The force field is described by the potential energy functions and its parameters.).

The methods that we will discuss use three strategies to reduce the computational burden resulting from the numerous possible arrangements of molecules in crystals: first, they use efficient search algorithms that tackle the complexity associated with the large number of arrangements of molecules. Second, they exploit experimental generalities that most organic molecules seem to crystallize in only a few symmetry groups, or that a crystal can be

* The use of empirical potential energy functions is a practical one. Calculations involving first principles, or quantum mechanics, are only appropriate for systems comprised of a few atoms.

† For example, if we allow a *single* rigid molecule to translate in all three directions within a 5 Å window (0.1 Å increments), and to rotate about all three axes within a 360° window (5° increments), then this molecule will have $50^3 \times 72^3$, or 4.7×10^{10} possible spatial configurations. This number dramatically increases if we consider more molecules, or if the molecules are conformationally flexible. In reality, this number is slightly less since it is known that organic molecules will tend to adopt only a few symmetries and will therefore eliminate some of these configurations[10].

decomposed into substructures, each of which is close to its global minimum in free energy. Third, they use supramolecular structures as the "molecular" unit.

The principle search algorithm used[164] involves Monte Carlo sampling of crystalline arrangements of molecules to find those that are plausible—that is, arrangements with low (favorable) values of U_{latt}. Monte Carlo algorithms, in the context of crystal engineering, generate crystalline structures by randomly changing the values of the crystalline lattice (a b, c, α, β, γ), and the geometry (primarily through torsions) or spatial orientation of the molecules. The value of U_{latt} of each newly generated crystalline structure is compared to that of the previous crystalline structure: If this new value of U_{latt} is lower than that of the previous structure, then this new crystalline structure is accepted. If this value of U_{latt} is higher than that of the previous structure, then the difference in these two values is weighted by a Boltzmann probability, and a random decision is made to keep or reject the new crystalline structure; the greater the difference in energies, the less probable that the new crystalline structure will be accepted. This procedure of generating and evaluating new crystalline structures is typically repeated many times (for example, on the order of 500 000 iterations) until the crystalline structure with the lowest value of U_{latt} is revealed.

Experimental generalities can help to guide strategies for predicting crystal structures. For example, most crystals of organic molecules contain a hierarchy of only a few structural motifs—one-dimensional stacks, two-dimensional layers, etc.[165]. Using these generalizations in a scheme for prediction helps to reduce the large number of crystalline arrangements of molecules by limiting the search to only a few symmetry types. Analogously, the use of supramolecular structures—for example, systems based on CA•M—as the basic structural unit that packs in a crystal reduces the degrees of freedom that are open to unconstrained molecules, and therefore significantly reduces the amount of computation involved[166].

The empirical force fields used in the computations reviewed here seemed adequate, but these force fields were only tested on a limited set of molecules: weaknesses appeared when polymorphism*, or extensive hydrogen bonding†, occurred. It is clear, therefore, that much work is still needed in improving the quality of these force fields to a level that makes them generally useful for crystal engineering.

Any procedure for predicting the crystalline state of organic molecules that must search the large number of spatial arrangements of molecules—even for crystals comprised of tapes based on the CA•M lattice—to find the

* This may or may not be a serious problem: some of these methods were able to correctly suggest that polymorphism might be present; although they could not distinguish which polymorph was the thermodynamically stable one.

† The hydrogen-bonding networks in the crystal structure of these compounds did not form the well-defined motifs of the types described in this review.

arrangement with the lowest U_{latt} can be computationally time consuming for even the simplest case. Fortunately, the methods discussed here demonstrate that predicting the crystal structures of some moderately complex organic molecules, based solely on their molecular structure, is becoming practical.

5.1 Generation of Clusters

Gavezotti developed a strategy for predicting the structure of organic crystals that relies on building a small cluster of two to four molecules using certain statistically favored space groups*. His method involves a systematic search to find the most energetically favorable arrangements of the molecules in this cluster[167]. Trial crystalline structures are then built by translating in space the most energetically favorable clusters, and determining which of these crystalline structures have favorable values of U_{latt}. Gavezzotti's method successfully predicted the crystalline structures of a variety of rigid hydrocarbons (the data were taken from the CSD)[61]. One shortcoming of his method is that in generating the cluster, no procedure is used that accounts for the effect of an infinite crystalline system (these procedures, which model the presence of surrounding unit cells, are referred to as "periodic boundary conditions"). The lack of periodic boundaries may limit the use of this method with compounds containing heteroatoms because the distance over which electrostatic interactions are important are typically greater than those explored in the small clusters examined in this method, and their omission may (or may not) compromise the predictive ability of this method.

Gavezzotti also discussed the difficulty in comparing crystal structures determined from different methods—that is, those from computation with those from experiments. For example, ambiguities can rise if two structures are compared based only on the parameters of the lattice (a, b, c, α, β, γ) which can be assigned arbitrarily. He suggests two more impartial metrics for comparing crystal structures: first, using the value of the distance between the centers-of-mass of molecules, and using the value of the difference in energies between a reference molecule and its neighbors; second, categorizing the "orientation of distinguishable molecular features in a crystal"—for example, the geometries of aromatic planes.

5.2 Generating Crystal Structures Using Simulated Annealing Monte Carlo in the Presence of Periodic Boundaries

Karfunkel and Gdanitz co-authored the first paper that demonstrated the successful prediction of crystal structures of organic molecules containing

* These spaces groups are comprised of translation, inverse, screw, and glide operations, and account for over 80% of all observable crystal structures in the Cambridge Crystallographic Database.

heteroatoms[168]. They used a simulated annealing Monte Carlo (SAMC) algorithm to optimize the structure of a crystal using a unit cell of arbitrary dimensions that contained a small number of molecules (1 to 4) under periodic boundary conditions. This algorithm uses high temperatures (usually values well above the temperature of sublimation for the crystal) in the initial stages of a MC procedure to increase the probability of accepting new crystalline arrangements of molecules that have values of U_{latt} that are more unfavorable relative to the previous arrangement. In this way, molecular arrangements in the crystal can escape a local minimum, and explore other minima. Karfunkel and Gdanitz eliminate "evaporation" of the molecules within the system caused by these high temperatures by constraining the molecules so that they cannot separate beyond a certain distance. The system is then "cooled" slowly over many cycles of computation to allow ample time to search for local minima. Variables in their method include the translational and rotational degrees of freedom for a molecule, torsions, and the appropriate lattice constants (a, b, c, α, β, γ). When analyzing the results from their computations, they eliminate ambiguities in comparing lattice vectors (as discussed by Gavezzotti) by converting the lattice vectors of each crystal structure to a common frame of reference (Niggli-reduced cell)[169]. Their implementation of SAMC is useful for rigid and semi-rigid molecules, but not yet general enough for conformationally flexible organic compounds. Their method has also proved useful for predicting crystalline structures containing just hydrocarbons[170].

Karfunkel and Gdanitz found that the choice of partial charges assigned to molecules containing heteroatoms was crucial for obtaining a predicted crystal structure that agreed with the experimental crystal structure: the electrostatic component of the potential energy was very sensitive to its choice of parameters. Also, Karfunkel *et al.* reported that the task of identifying similar crystal structures was not trivial, and therefore suggested that comparing the calculated X-ray powder diffraction patterns for crystal structures obtained from different computational methods may be the best means for comparing them[171].

5.3 Simulated Annealing Monte Carlo on Aggregates of Molecules in Conjunction with Principles of Crystals

Perlstein predicted the crystal structures of a number of organic molecules using a single molecule as the asymmetric unit[172,173]. He used a SAMC method similar to that of Karfunkel and Gdanitz; his approach to constructing the crystal, however, differed in the treatment of the crystalline environment, in that it closely follows the principles outlined by Kitaigorodsky[165]. These principles state that molecules initially assemble into one-dimensional aggregates; these aggregates then assemble into two-dimensional layers;

and finally these layers assemble to form the crystal structure in three dimensions. Perlstein titled these principles the "Kitaigorodsky Aufbau Principle" or KAP. Perlstein also bases his strategy on other experimental generalizations: only four types of symmetry in one-dimensional aggregates occur for 92% of all crystals (translation, inversion, screw, and glide)[174]; and only seven types of layers are formed form these aggregates[175]. Thus, Perlstein restricts his search to one-dimensional aggregates using only these four types of symmetry operators. When computing U_{latt}, Perlstein does not use periodic boundary conditions, but instead relies on molecular interactions between a central molecule and its nearest and next-nearest neighbors. More specifically, his approach uses SAMC to find one-dimensional stacks of molecules with the lowest U_{latt}, and then compares these molecular aggregates to those found in the crystal. This method works surprisingly well. Perlstein found that, for translational aggregates, the observed structure was less than 2 kcal/mol above the global minimum predicted for the aggregate; and for inversion, screw, and glide aggregates, the observed structure was less than 6 kcal/mol above the global minimum predicted for the aggregate.

5.4 Simulated Annealing Monte Carlo and Molecular Dynamics in Conjunction with Molecular Tapes

We have used computations to predict and rationalize the crystalline structure of molecular tapes comprised of hydrogen-bonded organic molecules. We believe that the restricted configurational freedom of molecular tapes, used in concert with existing computational methodologies, is a strategy that will give a good opportunity to predict the structures of organic molecular crystals. Our method for predicting crystal structures is similar to the SAMC method of Perlstein except that it allows the molecular tapes in the system to translate and rotate in three dimensions. Preliminary results from this work have focused on 4,5-disubstituted 2-benzimidazolones. We chose this class of cyclic ureas because they are conformationally more rigid, and therefore less prone to polymorphism, than many other organic molecules capable of forming hydrogen-bonded tapes[176]. As a class, these cyclic ureas often, but not invariably, form tapes[155]: when the substituents are large (iodine) or electronegative (fluorine) they instead adopt a three-dimensional motif[176]. If we *assume* that the cyclic ureas form tapes, we have successfully predicted the packing of tapes having methyl substituents based solely on the knowledge of the geometry of a single tape (Figure 5.48)[177]. Other computational methodologies—especially simulated annealing molecular dynamics (SAMD)[177,178]—also being explored for use in predicting crystal structures of these cyclic ureas: initial results are promising.

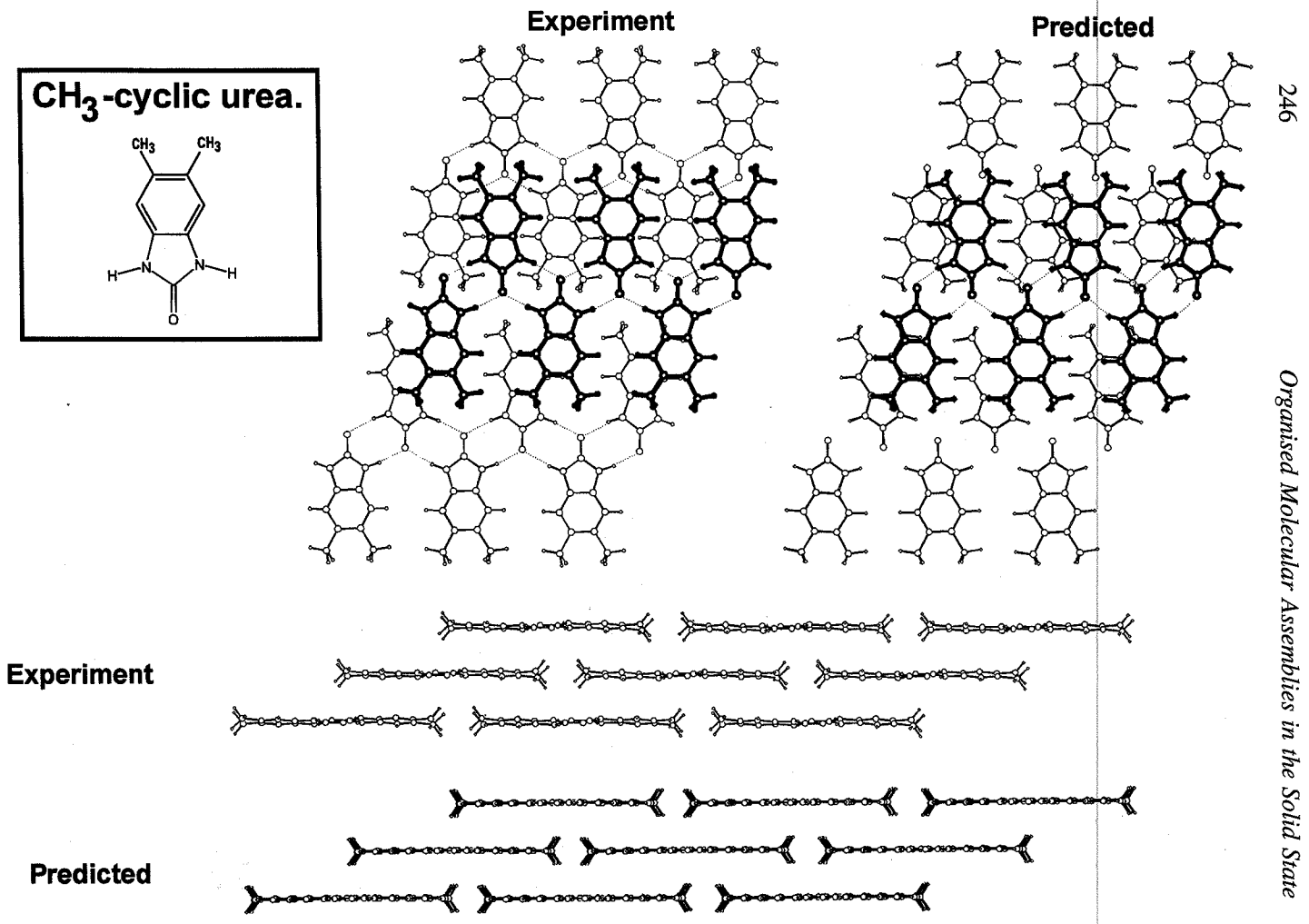

Figure 5.48 Computations successfully predicted the crystal structure of 4,5-dimethyl 2-benzimidazolone.

6. CONCLUSIONS

What is the outlook for the approaches to engineering the organic solid state suggested by the work reviewed in this chapter? The answer is, "Still uncertain". There is no doubt that the primary objective—designing and controlling the structures of crystals—is important: it is a broadly relevant problem in molecular recognition; it is a central intellectual challenge in solid-state chemistry; it offers possibilities for applications in areas from optoelectronics to drug-delivery systems. Despite the excellent work in the field, however, there has been no new dramatic advance in technique—such as that provided by the development of self-assembled monolayers in organic surface science, or the introduction of molecular beam epitaxy in semiconductor materials—that has rendered previously very difficult problems much easier.

The lack of revolutionary ideas notwithstanding, some areas of solid chemistry have seen very substantial advances in the last 20 years. X-ray crystallography of small organic molecules is now almost routine, and other techniques—such as solid state NMR spectroscopy and electron diffraction—have also contributed to the solution of structures in the solid state. These techniques have resulted in several crystallographic databases that provide a wealth of information about structure with which to formulate hypotheses. Based on these types of data, the work by Etter, Kitaigorodsky, Desiraju, Kennard, Dunitz and others has provided some very useful approaches to generalizations about the solid state. In our own work, the concepts of space filling and avoiding unfavorable steric interactions have proved to be especially useful approaches to simplifying design. the use of directional intermolecular interactions—such as hydrogen bonds—to limit the range of orientations open to molecules clearly simplifies the problem, and helps to make the goals of crystal engineering more approachable with present techniques. Very substantial difficulties still remain, however. Among them are the following:

- *Crystallization.* It remains difficult to grow diffraction-quality crystals of arbitrary organic compounds. As a result, crystallization is now the rate-limiting step in many investigations in this field, and until there are rapid ways of obtaining the structures of organic solids, the rate of progress in correlating molecular and crystalline structure will be slow.
- *Ranking crystalline arrangements.* The underlying problem is that organic molecules seem to be able to pack in a number of arrangements and conformations with similar energies. Every accessible conformation of a flexible organic molecule is, in principle, the basis of a new solid state structure. The overall energy of a crystal is the sum of many individual small interactions, and for this type of problem—as for the problem of molecular recognition of ligands by proteins—there are currently no search

routines that can sort the possible structures. Also, the problem of estimating the energies of different packing arrangements is too complex to be carried out by a system of simple rules, and computation will be necessary. Although the appropriateness of the commonly used potential functions is now well-established, computation is only just beginning to be useful in rationalizing known structures. Computation has, unfortunately, not yet reached the point of offering useful generalizations about organic molecules of even modest complexity.

- *Polymorphism.* The potential for polymorphism continues to cloud fundamental approaches to the energetics of crystals. There is no way of determining that there is not a lower energy polymorph than the one observed; measuring the thermochemical properties of crystals is difficult; and there is very little understanding of the processes governing the rates of crystal nucleation and growth.
- *Macroscopic properties.* The final objective of the field is to be able to predict the properties of organic crystals, and to design crystals having known properties. It is very difficult, however, to calculate properties accurately, even when the structure of the crystalline solid is known. To reliably predict properties reliably is still some years away.

7. ACKNOWLEDGMENTS

This project, and D.N.C., were supported by The National Science Foundation through Grant CHE-91-22331 to G.M.W., and by the Merck Corporation through a fellowship award to J.C.M.

8. REFERENCES

1. Lehn, J. M. *From Molecular to Supramolecular Nonlinear Optical Properties*, Vol. 455. American Chemical Society, Washington, DC (1991).
2. Ducharme, S., Scott, J. C., Twieg, R. J. and Moerner, W. E. *Phys. Rev. Lett.* **66**, 1846 (1991).
3. Günter, P. and Huignard, J. P. (eds) *Photorefractive Materials and Their Applications*, Vol. 1. Springer-Verlag, Berlin (1988).
4. Günter, P. and Huignard, J. P. (eds) *Photorefractive Materials and Their Applications*, Vol. 2. Springer-Verlag, Berlin (1989).
5. Byrn, S. R., Pfeiffer, R. R., Stephenson, G., Grant, D. J. W. and Gleason, W. B. *Chem. Mater.* **6**, 1148–1158 (1994).
6. Silverman, R. B. *The Organic Chemistry of Drug Design and Drug Action.* Academic Press, New York (1992).
7. Whitesides, G. M., Simanek, E. E., Mathais, J. P., Seto, C. T., Chin, D. N., Mammen, M. and Gordon, D. M. *Acc. Chem. Res.* **28**, 37–44 (1995).
8. Vogtle, F. *Supramolecular Chemistry.* John Wiley & Sons, New York (1991).

9. Ball, P. *Designing the Molecular World.* Princeton University Press, New Jersey (1994).
10. Bernstein, J. (ed.) *Polymorphism in Drug Design and Delivery*, pp. 203–215. Liss, New York (1988).
11. Bernstein, J. (ed.) *Polymorphism and the Investigation of Structure–Property Relations in Organic Solids*, pp. 6–26. Oxford University Press, Oxford (1991).
12. Bernstein, J. *J. Phys. D: Appl. Phys.* **26**, B66–B76. (1993).
13. Byrn, S. R. *Solid-State Chemistry of Drugs*. Academic Press, New York (1983).
14. Haleblian, J. K. *J. Pharmaceut. Sci.* **64**, 1269–1288 (1975).
15. McCrone, W. C. (ed.) *Polymorphism*, Vol. 2, pp. 725–767. John Wiley & Sons, New York (1965).
16. Bernstein, J. (ed.) *Conformational Polymorphism*, Vol. 32, pp. 471–518 . Elsevier, New York (1987).
17. Israelachvili, J. N. *Intermolecular and Surface Forces*. Academic Press, Orlando (1985).
18. Dunitz, J. D. and Bernstein, J. *Acc. Chem. Res.* **28**, 193 (1995).
19. Taylor, R. and Kennard, O. *Acc. Chem, Res.* **17**, 320 (1984).
20. Jeffrey, G. A. and Saenger, W. *Hydrogen Bonding in Biological Structures*. Springer-Verlag, Berlin (1991).
21. Vinogradov, S. N. and Linnel, R. H. *Hydrogen Bonding*. van Nostrand Reinhold, New York (1971).
22. Joesten, M. D. and Schaad, L. J. *Hydrogen Bonding*. M. Dekker, New York (1974).
23. Braga, D. and Grepioni, F. *Acc. Chem. Res.* **27**, 51 (1994).
24. Braga, D., Grepioni, F., Biradha, K., Pedireddi, V. R. and Desiraju, G. R. *J. Am. Chem. Soc.* **117**, 3156 (1995).
25. Desiraju, G. R. *Crystal Engineering: The Design of Organic Solids*, Vol. 54. Elsevier, New York (1989).
26. Desiraju, G. R. (ed.) *Organic Solid State Chemistry.* Elseveir, Amsterdam (1987).
27. Addadi. L., Berkovitch-Yellin, Z., Weissbuch, I., Mil, J. v., Shimon, L. J. W., Lahav, M. and Leiserowitz, L. *Angew. Chem., Int. Ed. Engl.* **24**, 466 (1985).
28. Wheeler, K. A. and Foxman, B. M. *Chem. Mater.* **6**, 1330 (1994).
29. Etter, M. C. *Isr. J. Chem.* **25**, 312–319 (1985).
30. Etter, M. C., MacDonald, J. C. and Bernstein, J. *Acta Crystallogr.* **B46**, 256–262 (1990).
31. Etter, M. C. *Acc. Chem. Res.* **23**, 120–126 (1990).
32. Bernstein, J., Etter, M. C. and MacDonald, J. C. *J. Chem. Soc., Perkin Trans.* **2**, 695–698 (1990).
33. Etter, M. C. *J. Phys. Chem.* **95**, 4601–4610 (1991).
34. Bernstein, J., Davis, R. E., Shimoni, L. and Chang, N.-L. *Angew. Chem. Int. Eng. Ed.* **34**, 1555–1573.
35. Leiserowitz, L. *Acta Crystallogr.* **B32**, 775–802 (1976).
36. Leiserowitz, L. and Schmidt, G. M. J. *J. Chem. Soc. A* 2372–2382 (1969).
37. Aakeröy, C. B., Hitchcock, P. B., Moyle, B. D. and Seddon, K. R. *J. Chem. Soc., Chem. Commun.* 1856 (1989).
38. Reutzel, S. M. and Etter, M. C. *J. Phys. Org. Chem.* **5**, 44–54 (1992).
39. Etter, M. C., Britton, D. and Reutzel, S. M. *Acta Crystallogr.* **C47**, 556–561 (1991).
40. Schwalbe, C. H., Williams, G. J. B. and Koetzle, T. F. *ACA Trans.* **23**, 101 (1987).
41. Etter, M. C., Urbanczyk-Lipkowska, Z., Zia-Ebrahimi, M. and Panunto, T. W. *J. Am. Chem. Soc* **112**, 8415–8426 (1990).
42. Etter, M. C. and Panunto, T. W. *J. Am. Chem. Soc.* **110**, 5896–5897 (1988).

43. Russell, V. A., Etter, M. C. and Ward, M. D. *J. Am. Chem. Soc.* **116**, 1941–1952 (1994).
44. Russell, V. A., Etter, M. C. and Ward, M. D. *Chem. Mater.* **6**, 1206–1217 (1994).
45. Etter, M. C. and Adsmond, D. A. *J. Chem. Soc., Chem. Commun.* 589–591 (1990).
46. Etter, M. C., Adsmond, D. A. and Britton, D. *Acta Crystallogr.* **C46**, 933–934 (1990).
47. Leiserowitz, L. *Acta Crystallogr.* **B33**, 2719–2733 (1977).
48. Etter, M. C., Huang, K. S., Frankenbach, G. M. and Adsmond, D. A. (eds) *Control of Symmetry and Asymmetry in Hydrogen-Bonded Nitroaniline Materials*, Vol. 455, pp. 446–456. Americal Chemical Society, Washington, DC (1991).
49. Etter, M. C., Frankenbach, G. M. and Adsmond, D. A. *Mol. Cryst. Liq. Cryst.* **187**, 25–39 (1990).
50. Etter, M. C. and Reutzel, S. M. *J. Am. Chem. Soc.* **113**, 2586–2598 (1991).
51. Wiedenfeld, H. and Knoch, F. *Acta Crystallogr.* **C46**, 1038 (1990).
52. Emsley, J., Reza, N. M. and Kuroda, R. *J. Cryst. Spectrosc.* **16**, 57 (1986).
53. Harkema, S. and Brake, J. H. M. t. *Acta Crystallogr.* **B35**, 1011 (1979).
54. Harkema, S., Bats, J. W., Weyenberg, A. M. and Feil, D. *Acta Crystallogr.* **B28**, 1646 (1972).
55. Etter, M. C. and Frankenbach, G. M. *Chem. Mater.* **1**, 10–12 (1989).
56. Hummel, G. J. v. and Helmholdt, R. B. *Acta Crystallogr.* **C47**, 213 (1991).
57. Benetollo, F., Bombieri, G. and Truter, M. R. *J. Heterocycl. Chem.* **26**, 981 (1989).
58. Harkema, S., Brake, J. H. M. t. and Helmholdt, R. B. *Acta Crystallogr.* **C40**, 1733 (1984).
59. Bernstein, J. *Acta Crystallogr.* **B35**, 360–366 (1979).
60. Boman, C.-E., Herbertsson, H. and Oskarsson, A. *Acta Crystallogr.* **B30**, 378–382 (1974).
61. Allen, F. H., Kennard, O. and Taylor, R. *Acc. Chem. Res.* **16**, 146–156 (1983).
62. Hart, H., Lin, L.-T. W. and Goldberg, I. *Mol. Cryst. Liq. Cryst.* **137**, 277–286 (1986).
63. Goldberg, I., Lin, L.-T. W. and Hart, H. J. *Incl. Phenom.* **2**, 377–389 (1984).
64. MacDonald, J. C. and Etter, M. C., Unpublished results.
65. Kuroda, Y., Taira, Z., Uno, T. and Osaki, K. *Cryst. Struct. Commun.* **4**, 321–324 (1975).
66. Matias, P. M., Jeffrey, G. A. and Ruble, J. R. *Acta Crystallogr.* **B44**, 516–522 (1988).
67. Craven, B. M., Vizzini, E. A. and Rodrigues, M. M. *Acta Crystallogr.* **B25**, 1978–1993 (1969).
68. Craven, B. M. and Vizzini, E. A. *Acta Crystallogr.* **B27**, 1917–1924 (1971).
69. Etter, M. C. and Huang, K.-S. *Chem. Mater.* **4**, 824–827 (1992).
70. Lechat, J. R., Santos, R. H. d. A. and Bueno, W. A. *Acta Crystallogr.* **B37**, 1468 (1981).
71. Lechat, J. R., Personal communication.
72. Prasad, P. N. and Williams, D. J. *Introduction to Nonlinear Optical Effects in Molecules and Polymers*. John Wiley & Sons, Inc., New York (1991).
73. Etter, M. C. and Baures, P. W. *J. Am. Chem. Soc.* **110**, 639–640 (1988).
74. Semmingsen, D. *Acta Chem, Scan.* **B28**, 169–174 (1974).
75. Singh, I. and Calvo, C. *Can. J. Chem.* **53**, 1046–1050 (1975).
76. Etter, M. C., Urbanczyk-Lipkowska, Z., Jahn, D. A. and Frye, J. S. *J. Am. Chem. Soc.* **108**, 5871–5876 (1986).
77. Etter, M. C., Parker, D. L., Ruberu, S. R., Panunto, T. W. and Britton, D. *J. Inclusion Phenom. Mol. Recogn. Chem.* **8**, 395–407 (1990).

78. Sarma, J. A. R. P. and Desiraju, G. R. *Acc. Chem. Res.* **19**, 222 (1986).
79. Ramamurthy, V. (ed.) *Photochemistry in Organized and Constrained Media.* VCH, New York (1991).
80. Goud, B. S., Panneerselvam, K., Zacharias, D. E. and Desiraju, G. R. *J. Chem. Soc. Perkin Trans.* II 325 (1995).
81. Dhurjati, M. S. K., Sarma, J. A. R. P. and Desiraju, G. R. *J. Chem. Soc., Chem. Commun.* 1702 (1991).
82. Desiraju, G. R. *Acc. Chem. Res.* **24**, 290 (1991).
83. Pedireddi, V. R. and Desiraju, G. R. *J. Chem. Soc., Chem. Commun.* 988 (1992).
84. Desiraju, G. R. *J. Chem. Soc., Chem. Commun.* 454 (1990).
85. Viswamitra, M. A., Radhakrishnan, R., Bandekar, J. and Desiraju. G. R. *J. Am. Chem. Soc.* **115**, 4868 (1993).
86. Desiraju, G. R. and Sharma, C. V. K. M. *J. Chem. Solc., Chem. Commun.* 1239 (1991).
87. Biradha, K., Sharma, C. V. K., Panneerselvam, K., Shimoni, L. C., Carrell, H. L., Zacharias, D. E. and Desiraju, G. R. *J. Chem. Soc., Chem. Commun.* 1473 (1993).
88. Sharma, C. V. K., Panneerselvam, K., Pilati, T. and Desiraju, G. R. *J. Chem. Soc., Chem. Commun.* 832 (1992).
89. Sharma, C. V. K., Panneerselvam, K., Pilati, T. and Desiraju, G. R. *J. Chem. Soc. Perkin Trans. II* 2209 (1993).
90. Desiraju, G. R., Murty, B. N. and Kishan, K. V. R. *Chem. Mater.* **2**, 447 (1990).
91. Thalladi, V. R., Panneerselvam, K., Carrell, C. J., Carrell, H. L. and Desiraju, G. R. *J. Chem. Soc., Chem. Commun.* 341 (1995).
92. Desiraju, G. R. and Kishan, K. V. R. *J. Am. Chem. Soc.* **111**, 4838 (1989).
93. Kishan, K. V. R. and Desiraju, G. R. *J. Org. Chem.* **52**, 4640 (1987).
94. Bertolasi, V., Nanni, L., Gilli, P., Ferretti, V., Gilli, G., Issa, Y. M. and Sherif, O. E. *New J. Chem.* **18**, 251 (1994).
95. Gilli, G., Bertolasi, V., Ferretti, V. and Gilli, P. *Acta Crystallogr.* **B49**, 564 (1993).
96. Bertolasi, V., Gilli, P., Ferretti, V. and Gilli, G. *J. Am. Chem. Soc.* **113**, 4917 (1991).
97. Gilli, G., Bellucci, F., Ferretti, V. and Bertolasi, V. J. *J. Am. Chem. Soc.* **111**, 1023 (1989).
98. Leiserowitz, L. *Acta Crystallogr.* **B32**, 775 (1976).
99. Leiserowitz, L. and Hagler, A. T. *Proc. R. Soc. London A* **388**, 133 (1983).
100. Subramanian, S., and Zaworotko, M. J. *Coord. Chem. Rev.* **137**, 357 (1994).
101. Bishop, R. and Dance, I. G. *Inclusion Compounds*, Vol. 4. Oxford University Press, Oxford (1991).
102. Ung, A. T., Bishop, R., Craig, D. C., Dance, I. G. and Scudder, M. L. *Chem. Mater.* **6**, 1269 (1994).
103. Bishop, R., Craig, D. C., Dance, I. G., Scudder, M. L., Marchand, A. P. and Wang, Y. *J. Chem. Soc. Perkin Trans.* II 937 (1993).
104. Ung, A. T., Bishop, R., Craig, D. C., Dance, I. G. and Scudder, M. L. *Tetrahedron* **49**, 639 (1993).
105. Ung, A. T., Bishop, R., Craig, D. C., Dance, I. G. and Scudder, M. L. *J. Chem. Soc. Perkin Trans.* II 861 (1992).
106. Ung, A. T., Bishop, R., Craig, D. C., Dance, I. G. and Scudder, M. L. *J. Chem. Soc., Chem, Commun.* 1012 (1991).
107. Atwood, J. L., Davies, J. E. D. and MacNicol, D. D. (eds). *Inclusion Compounds*, Vol 1–3. Academic Press, London (1984).
108. Aakeröy, C. B. and Seddon, K. R. *Chem. Soc. Rev.* **22**, 397 (1993).
109. Aakeröy, C. B. and Nieuwenhuyzen, M. *J. Am. Chem. Soc.* **116**, 10983 (1994).
110. Aakeröy, C. B. and Hitchcock, P. B. *Acta Crystallogr.* **C50**, 759 (1994).

111. Aakeröy, C. B., Hitchcock, P. B. and Seddon, K. R. *J. Chem. Soc., Chem. Commun.* **553**, (1992).
112. Aakeröy, C. B., Bahra, G. S., Hitchcock, P. B., Patell, Y. and Seddon, K. R. *J. Chem. Soc., Chem, Commun.* **152**, (1993).
113. Fan, E., Vicent, C., Geib, S. and Hamilton, A. D. *Chem. Mater.* **6**, 1113 (1994).
114. Garcia-Tellado, F., Geib, S. J., Goswami, S. and Hamilton, A. D. *J. Chem. Soc.* **113**, 9265 (1991).
115. Geib, S. J., Vicent, C., Fan, E. and Hamilton, A. D. *Angew. Chem. Int. Ed. Engl.* **32**, 119, (1993).
116. Geib, S. J., Hirst, S. C., Vicent, C. and Hamilton, A. D. *J. Chem. Soc., Chem. Commun.* 1283 (1991).
117. Lauher, J. W., Chang, Y.-L. and Fowler, F. W. *Mol. Cryst. Liq. Cryst.* **211**, 99 (1992).
118. Chang, Y.-L., West M.-A., Fowler, F. W. and Lauher, J. W. *J. Am. Chem. Soc.* **115**, 5991 (1993).
119. Zhao, X., Chang, Y.-L., Fowler, F. W. and Lauher, J. W. *J. Am. Chem. Soc.* **112**, 6627 (1990).
120. Toledo, L. M., Lauher, J. W. and Fowler, F. W. *Chem. Mater.* **6**, 1222 (1994).
121. Simard, M., Su, D. and Wuest, J. D. *J. Am. Chem. Soc.* **113**, 4696 (1991).
122. Wang, X., Simard, M. and Wuest, J. D. *J. Am. Chem. Soc.* **116**, 12119 (1994).
123. Ducharme, Y. and Wuest, J. D. *J. Org. Chem.* **53**, 5787 (1988).
124. Gallant, M., Viet, M. T. P. and Wuest, J. D. *J. Org. Chem.* **56**, 2284 (1991).
125. Russell, V. A., Etter, M. C. and Ward, M. D. *J. Am. Chem. Soc.* **116**, 1941 (1994).
126. Hollingsworth, M. D. and Palmer, A. R. *J. Am. Chem. Soc.* **115**, 5881 (1993).
127. Hollingsworth, M. D. and Cyr. N. *Mol. Cryst. Liq. Cryst.* **187**, 135 (1990).
128. Hollingsworth, M. D., Brown, M. E., Santarsiero, B. D., Huffman, J. C. and Goss, C. R. *Chem. Mater.* **6**, 1227 (1994).
129. Hollingsworth, M. D., Santarsiero, B. D. and Harris, K. D. M. *Angew. Chem. Int. Ed. Engl.* **33**, 649 (1994).
130. Hollingsworth, M. D., Santarsiero, B. D., Oumar-Mahamat, H. and Nichols, C. J. *Chem. Mater.* **3**, 23 (1991).
131. Gavezzotti, A. *Acta Crystallogr.* **B46**, 275 (1990).
132. Gavezzotti, A. *J. Am. Chem. Soc.* **105**, 5220 (1983).
133. Gavezzotti, A. New J. Chem. **6**, 443 (1982).
134. Zaworotko, M. J. *Chem. Soc. Rev.* **23**, 283 (1994).
135. Copp, S. B., Subramanian, S. and Zaworotko, M. J. *Angew. Chem. Int. Ed. Engl.* **32**, 706 (1993).
136. Copp, S. B., Subramanian, S. and Zaworotko, M. J. *J. Am. Chem. Soc.* **114**, 8719 (1992).
137. Christie, S. D., Subramanian, S., Thompson, L. K. and Zaworotko, M. J. *J. Chem, Soc., Chem. Commun.* 2563 (1994).
138. Subramanian, S. and Zaworotko, M. J. *Can. J. Chem.* **71**, 433 (1993).
139. Zerkowski, J. A., Seto, C. T., Wierda, D. A. and Whitesides, G. M. *J. Am. Chem. Soc.* **112**, 9025 (1990).
140. Wang, Y., Wei, B. and Wang, Q. *J. Cryst. Res.* **20**, 79 (1990).
141. Zerkowski, J. A. and Graham, R. Unpublished results.
142. Zerkowski, J. A., MacDonald, J. C., Seto, C. T., Wierda, D. A. and Whitesides, G. M. *J. Am. Chem. Soc.* **116**, 2382 (1994).
143. Zerkowski, J. A., Seto, C. T. and Whitesides, G. M. *J. Am. Chem. Soc.* **114**, 5473 (1992).
144. Zerkowski, J. A. and Whitesides, G. M. *J. Am. Chem. Soc.* **116**, 4298 (1994).

145. Zerkowski, J. A., Mathias, J. P. and Whitesides, G. M. *J. Am. Chem. Soc.* **116**, 4305 (1994).
146. Zerkowski, J. A., MacDonald, J. C. and Whitesides, G. M. *Chem. Mater.* **6**, 1250 (1994).
147. Simanek, E. E., Mammen, M., Gordon, D. M., Chin, D., Mathais, J. P., Seto, C. T. and Whitesides, G. M. *Tetrahedron* **51**, 607 (1995).
148. Bish, D. L. and Post, J. E. (eds) *Modern Powder Diffraction*. Mineralogical Society of America, Washington, DC (1989).
149. Klug, H. P. and Alexander, L. E. *X-Ray Diffraction Procedures*. John Wiley & Sons, New York (1954).
150. Etter, M. C. and Hoye, R. C. *Trans. Am. Crystallogr. Assoc.* **22**, 31 (1986).
151. Etter, M. C., Reutzel, S. M. and Vojta, G. M. *J. Mol. Struct.* **237**, 165 (1990).
152. Etter, M. C. and Vojta, G. M. *J. Mol. Graphics* **7**, 3–11 (1989).
153. Zerkowski, J. A., MacDonald, J. C. and Whitesides, G. M. *Chem. Mater.* **9**, 1933–1941 (1997).
154. Whitesides, G. M., Zerkowski, J. A., Macdonald, J. C. and Chin, D. N. *Mater. Res. Soc. Symp. Proc.* **328**, 3 (1994).
155. MacDonald, J. C. and Whitesides, G. M. *Chem. Rev.* **94**, 383–420 (1994).
156. Timofeeva, T. V., Chernikova, N. Yu. and Zorkii, P. M. *Russ. Chem. Rev.* **49**, 966 (1980).
157. Dauber, P. and Hagler, A. T. *Acc. Chem. Res.* **13**, 105–112 (1980).
158. Guo, Y., Karasawa, N. and Goddard, W. A. *Nature* **351**, 464–467 (1991).
159. Warshel, A. and Lifson, S. *J. Chem. Phys.* **53**, 582–589 (1970).
160. Lacks, D. J. and Rutledge, G. C. *J. Phys. Chem.* **98**, 1222–1231 (1994).
161. Karplus, M. and Kushick, J. N. *Macromolecules* **14**, 325–332 (1981).
162. Lipkowitz, F. and Boyd, D. B. (eds) *Reviews in Computational Chemistry.* VCH Publishers, New York (1990).
163. Kitaigorodsky, A. I. *Molecular Crystals and Molecules*, Vol. 29. Academic Press, New York (1973).
164. Allen, M. P. and Tildesley, D. J. *Computer Simulations of Liquids.* Oxford University Press, Oxford (1987).
165. Kitaigorodsky, A. I. *Organic Chemical Crystallography.* Consultants Bureau, New York (1961).
166. This idea is analogous to that for predicting the packing of rigid polymer chains: Segerman, E. *Acta Crystallogr.* **19**, 789 (1965).
167. Gavezzotti, A. *J. Am. Chem. Soc.* **113**, 4622–4629 (1991).
168. Karfunkel, H. R. and Gdanitz, R. J. *J. Comp. Chem.* **13**, 1171–1183 (1992).
169. Hahn, T. (ed.) *International Tables for Crystallography*, Vol. A. D. Reidel, Dordrecht (1983).
170. Gdanitz, R. J. *Chem. Phys. Lett.* **190**, 391–396 (1992).
171. Karfunkel, H. R., Rohde, B., Leusen, F. J. J., Gdanitz, R. J. and Rihs, G. *J. Comp. Chem.* **14**, 1125–1135 (1993).
172. Perlstein, J. *J. Am. Chem. Soc.* **114**, 1955–1963 (1992).
173. Perlstein, J. *J. Am. Chem. Soc.* **116**, 455–470 (1994).
174. Scaringe, R. P. and Perez, S. J. *J. Phys. Chem.* **91**, 2394–2403 (1987).
175. Scaringe, R. P. *Electron Crystallography of Organic Molecules.* Kluwer, Dordrecht (1990).
176. Schwiebert, K. E., Chin, D. N., MacDonald, J. C. and Whitesides, G. M. *J. Am. Chem. Soc.* **118**, 4018–4029 (1995).
177. Chin, D. N. MRS Transactions, Washington, 1998, in press.
178. Bruccoleri, R. E. and Karplus, M. *Biopolymers* **29**, 1847–1862 (1990).